Review of Inorganic Non-metallic Materials in Power Electronics Packaging Application

Chen, Junwei; Tian, Tiancheng; Gu, Chao; Zeng, Huidan; Hou, Fengze; Zhang, Guoqi; Fan, Jiajie

DOI
10.1109/TPEL.2025.3550882

Publication date
2025

Document Version
Final published version

Published in
IEEE Transactions on Power Electronics

Citation (APA)
Chen, J., Tian, T., Gu, C., Zeng, H., Hou, F., Zhang, G., & Fan, J. (2025). Review of Inorganic Non-metallic Materials in Power Electronics Packaging Application. *IEEE Transactions on Power Electronics*, *40*(8), 10509-10530. https://doi.org/10.1109/TPEL.2025.3550882

Review of Inorganic Nonmetallic Materials in Power Electronics Packaging Application

Junwei Chen, Tiancheng Tian, Chao Gu, Huidan Zeng, Fengze Hou, *Senior Member, IEEE*, Guoqi Zhang, *Fellow, IEEE*, and Jiajie Fan, *Senior Member, IEEE*

***Abstract*—Power electronics devices, pivotal in advancing electronic system technology, are essential for energy saving, enhancing power control efficiency, reducing noise, and minimizing size and volume. The evolution of power modules is based on innovative packaging structures, technologies, and materials. This article provides a comprehensive review of inorganic nonmetallic packaging materials and technologies in power electronics packaging. It first analyzes the packaging structures and trends of power electronics. The article then discusses inorganic nonmetallic encapsulants such as cement and glass in detail. It also reviews traditional ceramic substrates and elaborates on the advantages of multilayer ceramic technologies, including low-temperature co-fired ceramics, as substrates, while looking forward to the commercialization of inorganic composite substrates such as SiCp/Al matrix composites and diamond. Subsequently, the article overviews inorganic nonmetallic fillers for thermal interface materials, emphasizing the application of two-dimensional materials such as graphene and boron nitride, and introduces inorganic nonmetallic phase change materials. Finally, it explores the application and future development trends of inorganic nonmetallic materials in embedded packaging technologies.**

***Index Terms*—Embedded packaging technology, encapsulation materials, inorganic nonmetallic materials, power electronics packaging, substrate materials, thermal interface materials.**

I. Introduction

POWER electronic devices are essential components in contemporary electronic systems that enable the effective conversion of various types of electrical energy. High-power energy conversion equipment, such as those used in rail transportation, electromagnetic emission systems, renewable energy conversion, and smart grids, must operate under rapid response, high frequency, and transient conditions. These systems frequently encounter challenges such as high peak startup currents, prolonged fault operations, and complex multiphysics field coupling involving electrical, thermal, and mechanical elements [1], [2]. Wide bandgap (WBG) semiconductors, such as silicon carbide (SiC) devices, can push the output power of power conversion equipment to exceed the 100 MW level through organic series/parallel connections. Additionally, low-inductance packaging technology, which involves heterogeneous integration, supports the technical foundation for elevating the switching frequencies from hundreds of Hz to 10 MHz, thereby boosting the power density of the equipment [3], [4].

WBG power components surpass traditional silicon (Si), yet the latest generation of high-voltage, high-power devices faces challenges of doubled electrical stress, wider temperature fluctuations, more severe electromagnetic compatibility issues, and harsher thermal environments [5], [6]. The intensified coupling of electrical, magnetic, thermal, and mechanical stress fields has exacerbated the conditions, doubling the failure rate [3], [7]. The high failure rate of power devices stems primarily from the internal interconnection among various heterogeneous materials, involving electrical, thermal, and microscopic mechanical forces [6]. Externally, these devices encounter complex and variable operating conditions, such as radiation, humidity, and chemical corrosion [8], [9], [10]. Harsh environmental factors like high temperature and humidity can penetrate and diffuse into nonhermetic packaging materials (e.g., epoxy resin, silicone gel) with low glass transition temperatures (Tg), potentially leading to electrochemical corrosion and even the "popcorn" effect [10]. Even high radiation conditions can result in the degradation of the reliability of the die's oxide layer [11], [12]. In contrast, inorganic nonmetallic materials, with superior thermal stability, electrical insulation, and mechanical strength, are increasingly preferred for power device packaging [13]. These materials offer protection from mechanical, chemical and radiation hazards, enable heat dissipation, and ensure efficient signal and power distribution for optimal performance. Therefore, this work provides a comprehensive review of inorganic nonmetallic packaging materials for power electronics packaging. It compares the various technologies, materials, their advantages, and the main challenges encountered so far. Finally, potential future

Received 19 January 2025; accepted 8 March 2025. Date of publication 14 March 2025; date of current version 26 May 2025. This work was supported in part by the National Natural Science Foundation of China under Grant 52275559. Recommended for publication by Associate Editor K. Ngo. *(Corresponding author: Jiajie Fan.)*

Junwei Chen, Tiancheng Tian, Chao Gu, and Jiajie Fan are with the Institute of Future Lighting, Academy for Engineering & Technology, Shanghai Engineering Technology Research Center of SiC Power Device, Fudan University, Shanghai 200433, China (e-mail: chenjw24@m.fudan.edu.cn; 24110860049@m.fudan.edu.cn; 24110860040@m.fudan.edu.cn; jiajie_fan@fudan.edu.cn).

Huidan Zeng is with the School of Materials Science and Engineering, East China University of Science and Technology, Shanghai 200237, China (e-mail: hdzeng@ecust.edu.cn).

Fengze Hou is with the Institute of Microelectronics of Chinese Academy of Sciences, Beijing 100029, China (e-mail: houfengze@ime.ac.cn).

Guoqi Zhang is with the Department of Microelectronics Engineering, Delft University of Technology, 2628 CD Delft, The Netherlands (e-mail: g.q.zhang@tudelft.nl).

Color versions of one or more figures in this article are available at https://doi.org/10.1109/TPEL.2025.3550882.

Digital Object Identifier 10.1109/TPEL.2025.3550882

development directions are summarized, which can serve as a guide for future work in this field.

In this article, the organization is as follows. In Section II, the development trends of power electronics packaging materials and structures are reviewed. The different packaging forms of power devices, the inorganic nonmetallic packaging materials used, and future development trends are overviewed. In Section III, inorganic nonmetallic encapsulation materials (mainly cement and glass) are thoroughly surveyed. In Section IV, a comprehensive review of inorganic nonmetallic substrate materials for power electronics is provided. In Section V, the majority of existing inorganic nonmetallic fillers for thermal interface materials (TIMs) and phase change materials (PCMs) are discussed. In Section VI, the advantages, challenges, and potential development directions of embedded packaging technology are examined. Finally, Section VII concludes this article.

II. Power Electronics Packaging Materials and Structures Development Trends

The growing demand for high-efficiency, reliable, and lightweight equipment in industrial and energy systems has heightened the importance of power semiconductor devices operating at higher voltage and current levels [14], [15]. Traditional Si-based insulated-gate bipolar transistors (IGBTs) have nearly reached their theoretical performance limits. The new generation of semiconductor materials, which involves SiC-driven superior electrical and thermal performance, enables higher power density and reduced power loss [16]. By reducing thermal resistance (*R*th *J–C*) and increasing the maximum operating temperature (*Tj* max) of modules to exceed 200 °C, they enhance power density, current capability, and long-term reliability [4], [5], [17], [18], [19]. SiC MOSFETs, with their lower die area for a given ON-state resistance, result in reduced capacitance, giving them the potential for faster switching.

However, with the gradual maturity of new material power semiconductor devices such as SiC and GaN chips, as well as the development of more advanced chip technologies, the current power device packaging technologies are increasingly unable to meet the packaging requirements of these chip technologies. This trend limits the full potential of chip performance, such as operating temperature, short-circuit capability, switching speed, and efficiency. To overcome these challenges, design enhancements, such as Kelvin connections, orthogonal placement of power coupled with gate loops, and symmetrical layouts of power and gate circuits, improve performance and reliability [18], [19], [20]. However, packaging design usually emphasizes only electrical and thermal performance metrics within the device, including parasitic parameters and variations in temperature and pressure in real-world applications, which are often neglected. Consequently, maintaining consistent device performance across various scenarios becomes challenging. To address these issues, a range of advanced packaging materials and technologies, as well as packaging formats, are being developed and refined.

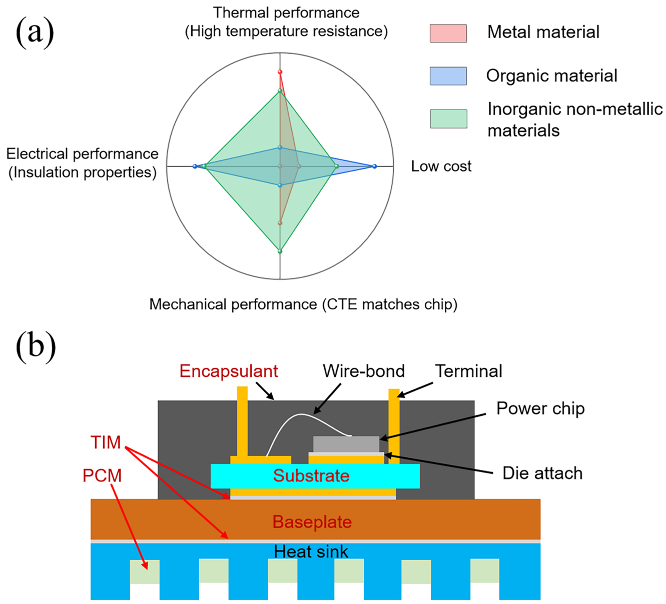

Fig. 1. (a) Relevant properties comparison of metals, organic materials, and inorganic nonmetallic packaging materials. (b) Schematic of a conventional packaging power device.

A. Power Electronics Packaging Materials

The performance of packaging materials largely determines the performance of power devices. The materials required for power devices are mainly categorized into metals, organic materials, and inorganic nonmetallic materials. With the advancement of power electronics technology, the requirements for the electrical, thermal, and mechanical properties of materials have become increasingly demanding. A comparison of the relevant properties is shown in Fig. 1(a) and a schematic of a conventional packaging power device is shown in Fig. 1(b). Metals, with their excellent electrical conductivity, play a crucial role in internal electrical interconnections, such as die attach materials, wire bonding, and gold stud bumps used for interconnections [21], [22], [23], [24], [25], [26]. In addition, the superior thermal conductivity of metals makes them ideal for use as power device frame materials and heat sinks. Organic materials, on the other hand, are widely used in encapsulants and TIMs due to their outstanding insulating properties, ease of processing, and bonding capabilities. Inorganic nonmetallic materials are renowned for their excellent mechanical properties and thermal stability. They are commonly used as substrate materials for power devices and have also found applications in encapsulants and thermal interface materials, among other areas.

B. Discrete Packaging

Discrete power devices, including power transistors, thyristors, MOSFETs, and IGBTs, are commonly used in medium and low-power applications, such as consumer electronics and industrial drives. Packaging options represented by TO-247, SOT227, D3PAK, and D2PAK are favored for their simplicity,

TABLE I
USE OF INORGANIC NONMETALLIC MATERIALS IN PACKAGING FOR DISCRETE POWER DEVICE

Device types	Sample types	Types of inorganic packaging material	Organization	Year	Ref.
Si MOS	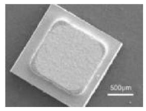	Passivation glass	East China University of Science and Technology	2024	[28]
SiC SBD	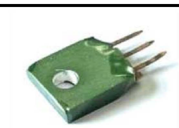	Encapsulation glass		2023	[29]
SiC SBD		Encapsulation cement	University of Central Florida	2008	[30]
Power transistor for GaN-SiC HEMT	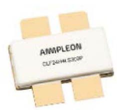	Ceramic shell	Ampleon (CLF24H4LS300P)		

cost-effectiveness, and versatility. Packaging choices depend on component type, application needs, thermal management, electrical properties, and hermetic sealing. Inorganic nonmetallic materials (see Table I), widely used for insulation in power devices, such as passivate P-N junctions with fused silicate glass, serve as encapsulants to isolate and protect the device environment. These materials, particularly in high-voltage and high-power rectifiers, outperform traditional polymers including e-resins and polyimides. Ceramic materials, known for their high insulation, thermal stability, and mechanical strength, are well-suited for shell packaging that requires mechanical support, environmental protection, and electrical connectivity in high-reliability electronics, such as those used in aerospace and military sectors [27]. Glass, valued for its excellent bonding capabilities, is also employed to seal bases and caps in cavity structures and metal can packages requiring airtightness. In extreme environments, involving space exploration and nuclear power, the integration of high-performance inorganic nonmetallic materials with simple, discrete device designs ensures reliable operation under high temperatures, radiation, and frequency bandwidth demands.

C. Module Packaging

Advancements in power device manufacturing technologies, processes, and packaging, are driving the evolution of power conversion equipment to address higher power requirements and more demanding operating conditions [17], [31]. Discrete power devices, which handle loads individually, face limitations due to their cooling capacity and material current-carrying limits. In high-voltage applications, elevated internal electric fields can easily lead to breakdown and failure. Consequently, power modules, which optimize the cost benefits of existing power devices through series and parallel configurations, have emerged as the preferred solution for high-power applications devices [32].

High-voltage devices consist of interconnected heterogeneous structures that integrate various materials. The conductive, thermal, and strain properties of these materials are closely interrelated. To boost power levels, it is crucial to enhance the maximum operating temperature of power chips, which involves advancements in high-melting-point semiconductor materials, high-temperature soldering technologies, and plastic encapsulation with a broad operating temperature range for chips and packaging. Most available SiC modules are advanced versions of Si-based IGBT modules. Infineon's PrimePACK modules have increased the number of parallel chips from 4 to 6, raising the current capacity from 450 to 1000 A. Additionally, the switching speed of internal chips has improved from tens of nanoseconds to a few nanoseconds to meet high power density and efficiency requirements. Infineon's easy modules demonstrate improved packaging density, being 60% smaller in volume [18], [19], [32], [33]. Table II illustrates new power module products and their performance, highlighting the application of inorganic nonmetallic material components in increasingly complex module structures. These advancements reflect a trend towards reduced inductance and thermal resistance. This shift indicates higher demands on packaging materials. As the power density and current levels of WBG semiconductors, including SiC and GaN, increase along with complex operating environments and impact loads, power devices encounter significant time-varying losses and thermal stress during their service life. These conditions can cause mechanical fatigue and damage to internal materials, leading to aging and potential failure of the device packaging structure [34], [35], [36].

III. ENCAPSULATION MATERIALS

Encapsulation materials are essential in power electronic modules, serving to isolate the internal and external environments of the module and prevent electrical breakdown, chemical corrosion, moisture infiltration, and harmful radiation [49].

TABLE II
USE OF INORGANIC NONMETALLIC MATERIALS IN ADVANCED POWER MODULE

Device types	Sample types	Dimension (mm)	Types of Inorganic packaging material	Inductance (nH)	Rth (°C/W)	Organization	Year	Ref.
DSC	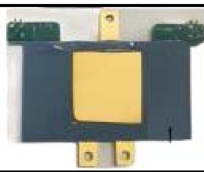	79.2× 66.4× 10.8	LTCC-derived interposer	2.3		University of Arkansas	2024	[37]
		34×40 × 1.13	Al_2O_3-DBC	1.3		Huazhong University of Science and Technology		[18]
	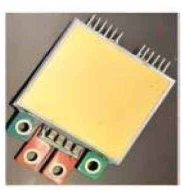	24 × 18 × 3.6	AlN-DBC	1.51		Stony Brook University		[38]
			AlN ceramic layer	0.93	0.073	University of Arkansas		[39]
			AlN-DBC	3	0.081	Huazhong University of Science and Technology	2022	[20]
	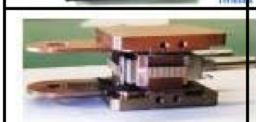		Al_2O_3-DBC	2.02		Xi'an Jiaotong University		[40]
	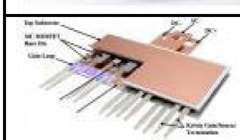		Si_3N_4-AMD	3.8		Xi'an Jiaotong University	2021	[41]
PCB embedded package			AlN baseplate	1.1		The Ohio State University	2020	[42]
	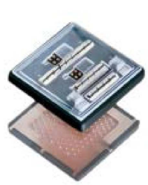		Multilayer ceramic substrate	≤ 1.6 nH		Fraunhofer Institute for Reliability and Microintegration	2019	[43]
	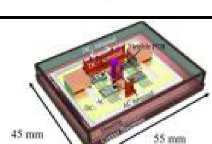	45×55	AlN-DBC	3.9		Virginia Polytechnic Institute and State University		[44]

TABLE II
(CONTINUED)

Device types	Sample types	Dimension (mm)	Types of Inorganic packaging material	Inductance (nH)	Rth (°C/W)	Organization	Year	Ref.
Hybrid Package	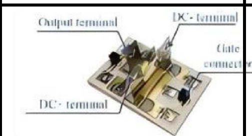		Al_2O_3-DBC	1.8		Huazhong University of Science and Technology	2020	[45]
	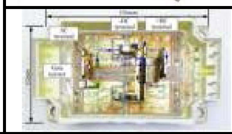	106×62	AlN-DBC	0.79		Huazhong University of Science and Technology	2018	[46]
SKiN			DBC	2.5		Semikron	2022	[21]
Other package			Cement-based encapsulation		0.453	Process Technology & Material Danfoss Si Power GmbH	2022	[47]
	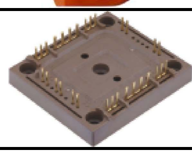	47.5× 52.6× 9.3	Si_3N_4-AMD		0.483 (simulated)	Microchip Technology Inc.	2020	[48]

They also minimize mechanical stress and impacts, thereby ensuring an effective insulation system for the module [50]. High-performance encapsulant materials should offer voltage isolation with a good dielectric strength (compared to air's 3 kV/mm), effectively suppress leakage currents with high electrical resistivity ($>10^{12}$ Ω), provide mechanical protection through an appropriate coefficient of thermal expansion (CTE) and modulus, and maintain thermal stability across suitable curing and application temperatures [51]. While polymers are commonly used for encapsulation, inorganic nonmetallic materials such as cement and glass can also be used in power device encapsulation [49], [52], [53].

A. *Polymer-Based Encapsulation Materials*

Epoxy resin is a traditional hard encapsulation material widely used in electronic packaging due to its excellent adhesion strength and chemical resistance. The glass transition temperature (Tg) of epoxy molding compound (EMC) typically ranges from 125 to 175 °C, which is a key parameter for evaluating thermal stability. For power modules, the maximum operating temperature should generally be kept below the Tg of the encapsulant. To address the low Tg and poor thermal stability of epoxy resin, inorganic fillers can be added to create efficient thermal paths, improving heat dissipation. However, this may introduce defects and cause issues such as poor processability and higher manufacturing costs as the filler content increases. For example, when using dicyclopentadiene and naphthalene epoxy resin with an acid anhydride hardener to implement cross-linking reactions, it is possible to achieve a high cross-link density, raising the Tg above 270 °C [54]. However, this may negatively impact flowability and increase water absorption. Higher cross-link densities also require higher curing temperatures (e.g., over 300 °C for polyimide), which can increase the material's brittleness and reduce its toughness. Therefore, improving the high-temperature performance of epoxy resin often comes at the cost of reduced processability and durability.

Silicone gel, on the other hand, is a soft encapsulant known for its ability to recover from damage caused by mechanical stress or electrical degradation, such as electrical treeing [55], [56]. However, its low Tg (below −60°C) means that its thermal performance is mainly assessed by the onset temperature of degradation. Commercial silicone gel typically remains stable between −45 and 200°C. The high CTE of silicone gel (>100 ppm/°C) can create a risk of lead detachment under thermal stress, although its low modulus helps mitigate this risk to some extent. However, it also introduces mechanical wear issues. Furthermore, silicone gel is moisture-sensitive, meaning that careful thickness design is crucial for ensuring a crack-free lifetime, and it also affects both heat dissipation and adhesion. The addition of inorganic nonmetallic fillers can reduce CTE, control partial discharge, and lower the electric field, but these improvements come with similar issues to those encountered with epoxy resin. To enhance thermal stability, high-temperature nonpolar dibenzyltoluene liquid could be considered as a substitute [54]. These insulating liquids offer good thermal and dielectric performance but lack the mechanical support required to protect power module components, necessitating additional design or material considerations.

WBG semiconductor materials enable devices to operate under high temperature and power conditions. However, polymer-based encapsulation materials often fall short in high-temperature performance, limiting device improvements. In contrast, inorganic nonmetallic materials, known for their robust thermal stability, are therefore preferred for high-temperature encapsulation materials [50], [57].

B. Cement-Based Encapsulation Materials

Cement, a hydraulically setting inorganic binder material often known as wet-setting ceramics, offers several benefits including high-temperature resistance (> 1000 °C), high thermal conductivity (0.58–6 W·m^{-1}·°C^{-1}), good chemical stability, high flowability, strong plasticity, ease of processing, and low cost. The University of Central Florida used hydro-set ceramic materials (Cermacast 673N) to develop a 2×2 mm^2 SiC Schottky diode prototype, which operated normally at 300 °C [30]. The Air Force Research Laboratory encapsulated SiC power modules with ceramic-filled adhesives (Resbond 919 and 920), which successfully passed thermal shock tests (–55 to 200 °C) and high-temperature reverse bias tests (2 kV and 250 °C) [58]. Kaessner et al. [59] at the University of Tuebingen investigated calcium aluminate cement (CCC) encapsulation materials, consisting of an iron-free calcium aluminate cement (CAC) matrix and alumina. However, the high pH value of this cement corroded the metal layer on the chip surface, causing the devices to fail reliability tests. Consequently, Kaessner employed a ceramic encapsulation material (CE) with a hydratable alumina matrix and alumina filler particles with a lower pH value. This material successfully encapsulated custom power modules—featuring Semikron CAL diodes and Infineon IGBT4s soldered onto a DCB substrate—using a special curing process at 60 and 150 °C for 3 h each. The devices passed high temperature reverse bias (HTRB) test [60]. Fudan University enhanced the thermal conductivity of cement composite encapsulation materials by incorporating Al_2O_3 fillers into CAC and utilized a finite element model (FEM) to predict the thermal conductivity of various filler composites, streamlining the development process [61]. Concurrently, Kaessner et al. [59] employed phosphate cement (PC) to encapsulate Mini power modules (MiniPIM, Danfoss Silicon Power), featuring two direct bonded copper ceramic (DBC) substrates soldered onto a standard copper baseplate, each substrate with two IGBTs and two diodes connected via solder joints and Al-wire bonding. These devices excelled in reliability tests, passing HTRB and high voltage-high humidity high temperature reverse bias tests and enduring 70 000 power cycles, which is 3.5 times longer than conventional Si-encased modules. Additionally, the Fraunhofer Institute for Microstructure of Materials and Systems assessed the effects of cement encapsulation on the Econo3 power module using numerical methods. The results demonstrate enhanced reliability

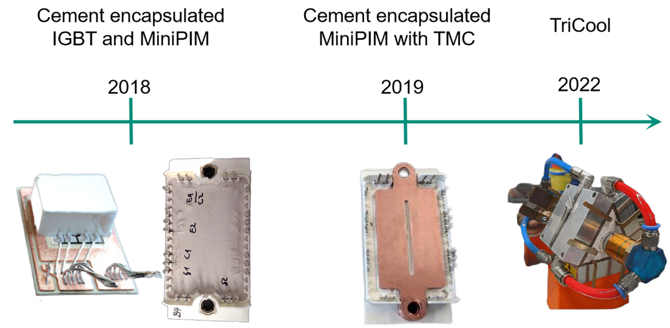

Fig. 2. Overview of the process of main developing cement encapsulation materials [47], [59], [60], [63]. Reproduced with permission. IEEE, copyright 2018, IEEE, copyright 2019 Elsevier Ltd.

in PC-cement-encapsulated power modules [62]. Kaessner, in collaboration with FuE-Zentrum Fachhochschule Kiel GmbH, enhanced the design by adding a copper layer thermal mass circuit (TMC) atop the cement-encapsulated modules, which connected to the heat sink. Test results reveal that, compared to modules using only CE materials, the TMC structure reduces the maximum inlet coolant temperature (*Ti*) by 7.6 °C and lowers the junction temperature (*Tj*) by 12.9 °C compared to the results in [63]. Kaessner later introduced the TriCool module concept, featuring CE cement encapsulation material [47]. The TriCool module includes three base units with central coolant inflow and return, each featuring a 3-mm Cu bottom plate. The adjacent bottom plates' DBCs connect via internal and external busbars, enabling water cooling in the central return zone [47]. Unlike TMC, the TriCool design offers a fully restructured module body with a triangular shape, significantly lowering *Tj* and *R*th. Compared to standard CE material modules, the TriCool achieves a 24.96 °C reduction in *Tj* and a 28.94% decrease in *R*th. The main development process of cement encapsulation materials is depicted in Fig. 2.

C. Glass-Based Encapsulation Materials

Glass is a promising inorganic high-temperature encapsulation material, which offers adjustable softening temperature, sintering temperature, as well as thermal expansion coefficient (CTE). Its exceptional thermodynamic and chemical stability, coupled with excellent electrical insulation, durability, and mechanical strength, makes it highly suitable for high-power module applications.

Liu et al. [64] at Virginia Tech initially evaluated the compatibility of lead glass powder (Ceradyne, Inc.) with DBC substrates. They encapsulated a DBC substrate with electrodes using molten glass at 500 °C directly and compared the samples with those encased in commercial polymer materials, maintaining them at 250 °C for 1000 h. The results indicated that the partial discharge inception voltage (PDIV) of the polymer-encapsulated samples dropped over 80% within 100–200 h, while the glass-encapsulated samples retained a high breakdown field strength of 4.5 kV after 1000 h [64], [65]. However, a self-made SiC MOSFET module, encapsulated with the same method, experienced performance degradation due to damage to the MOSFET's

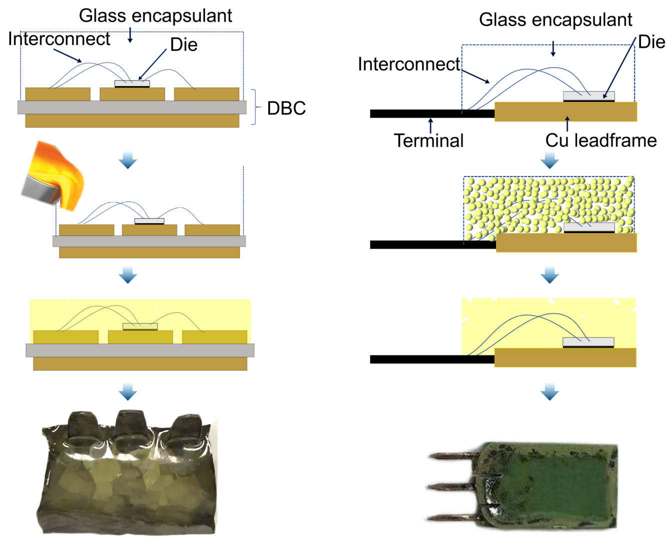

Fig. 3. Overview of the processes and comparisons of two different glass encapsulation techniques [64], [67]. Reproduced with permission. copyright 2021, IEEE, copyright 2025 Elsevier Ltd.

oxide layer. To mitigate the thermal-mechanical stress from the differing CTEs of glass and DBC during cooling, the team introduced a polyimide (PI) layer between the glass and chip. The static characteristics of the glass-encapsulated samples aligned with the device datasheet values. Despite the PI buffer layer reducing interface stress, micropores could still lower PDIV. To resolve this problem, the team developed a buffer layer using a nonlinear resistive polymer-nanoparticle composite material, which improved insulation without affecting thermal performance [66]. Researchers from East China University of Science and Technology and Fudan University addressed the issue by altering the BaO and ZnO ratios in bismuth-based glass. This modification reduced the encapsulation temperature while preserving excellent insulation properties [29]. They used a sealing technique at 475 °C with glass powder to successfully encapsulate a TO-247 SiC Schottky barrier diode (SBD) [29]. However, the issues of high packaging temperature (475 °C for 35 min) and high CTE (= 11.48 ppm/°C) persisted. Subsequently, the team incorporated $PbTiO_3$ ceramic powder to adjust the CTE of the glass-based encapsulating material for SiC power devices, using a process at 450 °C. The encapsulated device passed static performance tests with a low thermal resistance of 0.45 °C/W, maintaining excellent performance even after 1176 h of high-temperature aging and remaining nearly unchanged throughout thermal cycling between temperatures of –50 to 150 °C for 100 cycles [67]. Unlike traditional encapsulation materials with low thermal stability (< 200 °C), glass-encapsulated SiC devices can function at temperatures up to 300 °C. The methods and comparative results of the two different glass encapsulation techniques are illustrated in Fig. 3.

As the junction temperature of wide-bandgap power devices continues to increase, the limitations of polymer encapsulation materials become more apparent, particularly in terms of thermal management and thermo-mechanical robustness. Inorganic nonmetallic materials offer a promising solution to this challenge. However, ceramic materials, which typically require high sintering temperatures, are not viable options for encapsulation. Instead, cement and glass stand out due to their favorable processability, thermal, and electrical properties. Moreover, both cement and glass are traditional radiation shielding materials, making them highly suitable for applications in high-radiation environments, such as deep space exploration and nuclear power plants, where device reliability is crucial [68], [69]. Despite their potential, using cement and glass as encapsulation materials for power devices presents several challenges. For cement, the porous structure weakens electrical insulation and corrosion resistance, which can reduce device performance, particularly in high-humidity environments. Additionally, the alkaline hydration process can lead to electrochemical reactions, resulting in electrical failures. Cement's poor adhesion to other materials often necessitates high-temperature-induced dehydration or the use of additional coatings to improve bonding. Glass, on the other hand, presents challenges such as high processing temperatures (over 450 °C) and thermal-mechanical stress due to mismatched CTE with the substrate. Furthermore, its high dielectric constant (8–12) and relatively high Young's modulus (58 GPa) complicate its use in power device applications [70]. To address these issues, solutions such as incorporating a buffer layer between the glass encapsulant and the ceramic substrate have been proposed [71], [72]. Another approach involves modifying the glass's intrinsic properties to reduce its softening temperature, CTE, and Young's modulus. Although cement and glass encapsulation materials generally exhibit relatively low thermal conductivity, their thermal performance remains superior to that of conventional polymer-based encapsulants available on the market. Raw materials for these inorganic encapsulants are easily sourced from traditional suppliers, but packaging equipment often requires significant upgrades or redesigns to accommodate these materials effectively. Continued research and development are essential to overcoming these challenges and ensuring the broader application of cement and glass as encapsulants in power devices.

IV. Substrate Materials

In power module packaging, substrates serve as both mechanical support for power chips and dielectric layers for electrical insulation of circuits while facilitating thermal management for active devices [73], [74]. However, existing organic substrate materials face notable drawbacks, including high thermal expansion (CTE) coefficients, warping, excessive shrinkage, and insufficient temperature resistance, making them unsuitable for the higher junction temperatures of next-generation WBG power devices. Consequently, adopting inorganic nonmetallic materials as dielectric barrier layers to meet more stringent thermal demands has gained importance [75]. Ceramic substrates are commonly used in high-performance, high I/O density products due to their excellent CTE compatibility with power chip materials and strong reliability under high-temperature processing or application conditions. However, inorganic nonmetallic substrate materials are preferred for power chips because they offer

TABLE III
COMPARISON OF TRADITIONAL CERAMIC SUBSTRATES AND PROPERTIES

Types	Materials/ Merchants	CTE (ppm/°C)	Thermal conductivity (W·m^{-1}·°C^{-1})	Heat tolerance (°C)	Redistribution layer materials	Advantages	Disadvantages
TFC	Al_2O_3	7–9	20–30	300	Au, Ag, Cu	Technically advanced, straightforward process, and cost-effective.	Surface roughness and misalignment
	AlN	4.2–7	120–200				
DBC	Al_2O_3	7–9	20–30	500	Cu	Accurate alignment, no sintering shrinkage, and differential issues.	Copper foil is excessively thick and requires processing.
	AlN	4.2–7	120–200				
DPC	Al_2O_3	7–9	20–30	<300	Cu	Accurate alignment, no sintering shrinkage, no differential issues, and capable of producing 10–50 μm lines.	The copper layer is too thin and needs electroplating to increase its thickness.
	AlN	4.2–7	120–200				
AMB	Al_2O_3	7–9	20–30	<400	Cu	Accurate alignment, no sintering shrinkage, no differential issues, and capable of producing 10–50 μm lines with good thermal conductivity and high reliability.	Requires electroplating to thicken, incurs high costs, requires limited suitable active solders, and the solder's composition and process crucially affect the welding quality.
	AlN	4.2–7	120–200				
	Si_3N_4	2.7–4.5	40–100				

superior mechanical support, thermal stability, electrical insulation, and shielding properties. As power modules evolve with increased integration, power density, and operating frequency, the challenge of meeting the electronic industry's varied demands for thermal conductivity, mechanical strength, and dielectric properties with a single material has led to the development of composite substrates that combine the advantages of different materials to meet these evolving needs.

A. Conventional Ceramic Substrate

Inorganic nonmetallic materials such as Al_2O_3, BeO, AlN, and Si_3N_4 are widely utilized in power module packaging through advanced packaging technologies including thick film ceramic substrate (TFC), DBC, active metal brazing (AMB), and direct-plated copper ceramic substrate (DPC). Table III presents common substrate performances [76]. Each method has distinct advantages. TFC substrates are economical and simple to produce but have limited current-carrying capacity due to their thin metal layers (< 1 μm), making them unsuitable for high-power devices. DPC substrates enable low-temperature processing (around 300 °C), reducing circuit damage risk; however, their performance depends heavily on process accuracy. DBC substrates provide superior thermal conductivity and stability in high-power applications, making them prevalent in IGBT production. However, they are susceptible to thermal stress and copper delamination due to mismatched thermal expansion coefficients. AMB substrates address these issues by bonding thicker copper layers at lower temperatures using active metal solders. This approach enhances compatibility with Si_3N_4 and SiC materials and shows potential for applications involving SiC semiconductors. However, AMB's use of rare-earth elements in solders presents storage and handling challenges. After fabrication, all ceramic substrates require metallization and surface patterning through image transfer technology for electrical connections. The electroplating process, however, demands strict environmental controls. Recently, resource recovery and closed-loop systems have become key trends in pollution control within the electroplating industry.

B. High-Temperature Co-Fired Ceramics (HTCC)

With advancements in power device manufacturing technologies, processes, and packaging, power conversion equipment is increasingly capable of handling higher power levels and more demanding operating conditions. Conventional PCB substrates, including FR4 and high-performance polytetrafluoroethylene, are inadequate for power modules used in harsh environments and high-reliability applications. High-temperature co-fired ceramics (HTCC) and low-temperature co-fired ceramics (LTCC), integral to multilayer ceramic technology, facilitate the layering of multiple dielectric and metal layers. They incorporate distributed and staggered via holes, allowing the creation of complex multilayer structures with embedded cavities and components. This advancement enables device miniaturization and high-frequency applications, providing significant design flexibility and facilitating the production of new power modules. Performance data for typical application products are detailed in Table IV [73].

HTCC is usually composed of high thermal conductivity ceramic powders such as AlN or Si_3N_4, processed through tape casting and cofired at temperatures exceeding 1350 °C. The thermal conductivity of the composite material ranges from 20–200 W·m^{-1}·°C^{-1}, depending on the composition and purity of the ceramic powders. Researchers at Huazhong University of Science and Technology tackled challenges related to bonding wires in conventional packaging designs, including elevated parasitic inductance, inadequate high-temperature performance, and substantial thermal–mechanical stress. Fig. 4(a) illustrates their proposed robust, high-temperature-resistant packaging design based on HTCC that omits bonding wires, reducing stress

TABLE IV
COMPARISON OF DIFFERENT MULTILAYER CERAMIC SUBSTRATES AND THEIR PROPERTIES

<table>
<tr><th>Types</th><th>Materials/ merchants</th><th>CTE (ppm/°C)</th><th>Thermal conductivity ($W \cdot m^{-1} \cdot °C^{-1}$)</th><th>Heat tolerance (°C)</th><th>Redistribution layer materials</th><th>Advantages</th><th>Disadvantages</th></tr>
<tr><td>HTCC</td><td>AlN</td><td>–</td><td>16–24</td><td>1000</td><td>W, Mo, Mn</td><td>The process is well-established and cost-effective.</td><td>Alignment accuracy is low, the circuit surface is rough, and the high sintering temperature results in substantial energy consumption.</td></tr>
<tr><td rowspan="4">LTCC</td><td>Al_2O_3</td><td>7.1</td><td>2–3</td><td rowspan="4">850</td><td rowspan="4">Au, Ag, Cu</td><td rowspan="4">The process is proven, offering high electrical performance and adjustable performance.</td><td rowspan="4">Low alignment precision, rough circuit surface, and surface shrinkage.</td></tr>
<tr><td>DuPont 9K7</td><td>4.4</td><td>4.6</td></tr>
<tr><td>Ferro A6M</td><td>7</td><td>2</td></tr>
<tr><td>Heraeus HL200</td><td>6.1</td><td>2.6</td></tr>
<tr><td rowspan="3">ULTCC</td><td>muLtcc40</td><td>4.5</td><td></td><td>480</td><td rowspan="3">Al, nanosilver</td><td rowspan="3">Cost-effective and energy-efficient.</td><td rowspan="3">Inappropriate materials and weak dielectric properties.</td></tr>
<tr><td>TiO_2A-30GO17</td><td>7.4</td><td></td><td rowspan="2">400</td></tr>
<tr><td>TiO_2R-30GO17</td><td>8.3</td><td></td></tr>
</table>

and enhancing overall reliability [74]. However, the elevated sintering temperature of HTCC constrains the selection of metallic conductor materials, primarily limiting them to metals with high melting but lower conductivity points, such as tungsten, molybdenum, and manganese. Consequently, HTCC is better suited for manufacturing passive components, such as high-temperature-resistant resistors and capacitors, within wide-bandgap power modules.

C. Low-Temperature Co-Fired Ceramics (LTCC)

LTCC achieves a sintering temperature below 900 °C by incorporating 30–50% low-melting-point glass into the raw porcelain belt. This strength allows the use of materials with superior electrical conductivity, such as gold, silver, and copper, for electrodes and wiring. LTCC modules are distinguished by their compact design, outstanding mechanical and thermal shock resistance, and exceptional electrical performance, including dielectric loss several orders of magnitude lower than that of RF4 [77]. Consequently, LTCC is unmatched in high-frequency applications, with no organic material matching its performance in frequency, size, and cost. One straightforward manufacturing method for LTCC power modules is surface mount device (SMD) technology. The Electronics and Telecommunications Research Institute first utilized SMD technology for packaging SiC SBDs within multilayer ceramics. They embedded bare SiC SBD chips into the LTCC substrate cavities and employed flat Cu clip bonding to minimize parasitic inductance [see Fig. 4(b)] [75]. Compared to conventional TO-220 package products, this approach reduces the parasitic inductance (Q_rr) by 18.7% and outperforms commercial SMD SiC SBD products in efficiency and thermal performance [see Fig. 4(c)] [76]. Similar technology has also been implemented in the manufacture of power inductors [78]. The Fraunhofer Institute for Ceramic Technologies and Systems and Integrated Systems and Device Technology developed a new packaging concept that integrated power semiconductor devices into LTCC using a combination of silver foil and solid body integration, to enhance the operational temperature of SiC power devices to over 400 °C [79]. By employing pressure-assisted sintering and constraining sacrificial layers, the lateral shrinkage of LTCC material was eliminated, allowing the successful integration of SiC devices into commercial LTCC substrates. The electrical interconnections of the embedded SiC chips were then validated by measuring the resistance between the top and bottom of the LTCC pre-packaged module [see Fig. 4(d)–(f)] [80], [81]. Additionally, new techniques for embedding SiC devices into ultralow-temperature co-fired ceramics (ULTCC), which can be sintered at 500 °C, are explored as an alternative due to LTCC's higher sintering temperature [82]. Embedded LTCC technology is a highly effective packaging solution for protecting electronic devices from high temperatures and corrosive gases. The LTCC-

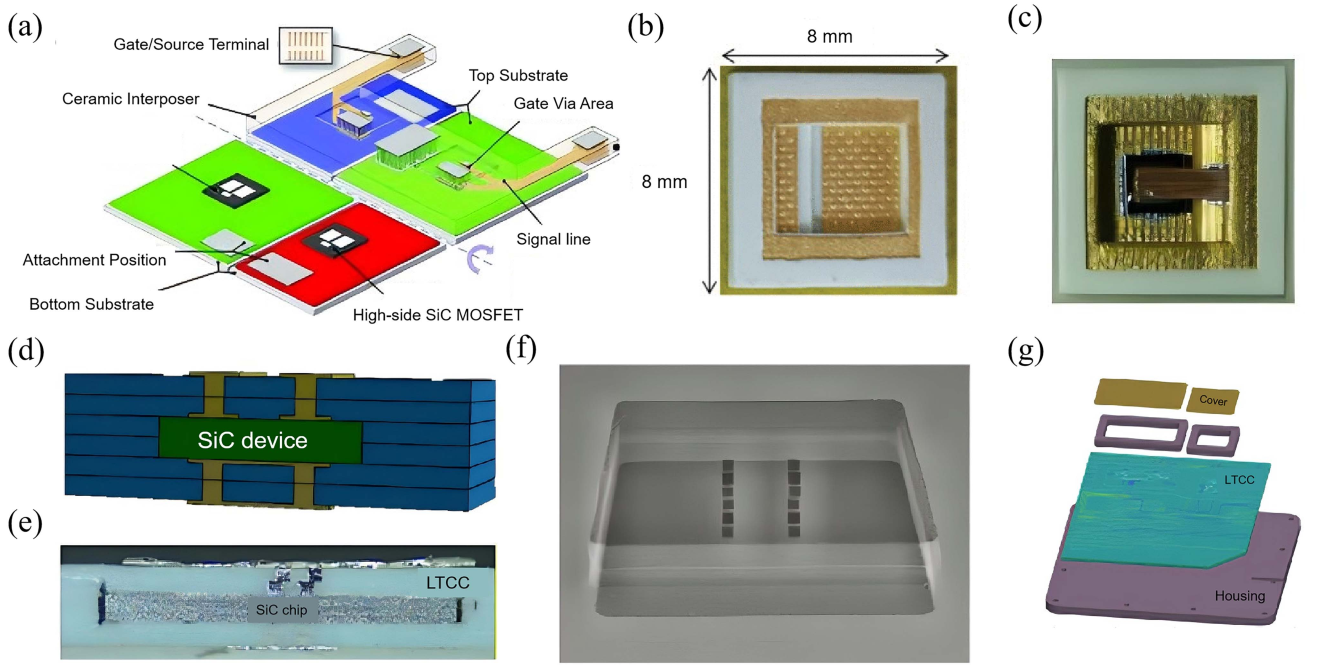

Fig. 4. Power device featuring an multilayer ceramic substrate. (a) Internal photographs of the power module based on HTCC packaging structure. (b) Internal photographs of the fabricated leadless LTCC-based SiC SBD SMD package. (c) Embedding a SiC semiconductor device in a premetallized LTCC multilayer. (d) Embedding a SiC device in a pre-metallized LTCC multilayer stack, cross-sectional view. (e) X-ray image. (f) and (g) LTCC-based all-in-one CAMP package [75], [80], [81], [82], [84]. Reproduced with permission. copyright 2024, IEEE, copyright 2020, IEEE, copyright 2020, IEEE, copyright 2023, IEEE, copyright 2022 Elsevier Ltd., copyright 2022 cnki.

based interposer provides a robust structure, electrical isolation, and ease of fabrication [37]. Recently, advancements in space technologies utilizing WBG semiconductor materials such as gallium nitride (GaN) and GaN-based alloys have prompted research into solid-state power amplifiers (SSPA) as alternatives to traveling wave tube amplifiers [83], [84]. The China Academy of Space Technology (Xi'an) integrated packaging technology to develop a GaN-based SSPA using a phase-shift-full-bridge topology, showcasing LTCC's capability to support deep space exploration with WBG power modules [see Fig. 4(g)] [84]. Due to its numerous advantages, LTCC is extensively used in the manufacture of automotive power electronics. Delco Electronics, a General Motors subsidiary, utilizes LTCC technology to manufacture engine control modules, while Magneti Marelli's Electronics in Italy employs it for automotive oil valve control modules incorporating power MOS devices.

Although LTCC provides notable benefits for power module packaging, it also has some limitations. The high glass content in the LTCC raw porcelain belt results in a relatively low thermal conductivity, potentially impacting the reliability of high-density LTCC modules. To mitigate this issue, researchers often incorporate high thermal conductivity ceramics such as Si_3N_4, BN, and diamond into the raw porcelain belt, and optimize the material's electrical performance with advanced microcrystalline glass [85]. For LTCC processes, thermal vias offer an effective thermal management solution. This technique involves creating vertical vias under heat sources in integrated LTCC devices and cofiring them with high thermal conductivity materials involving silver (Ag), silver-palladium (AgPd), and platinum (Pt). This method enables efficient heat transfer to heat sinks or the device exterior [86], enhances heat dissipation efficiency, and maintains the device's thermal stability. Future developments in LTCC technology will focus on improving heat dissipation performance, lowering sintering temperatures through the ULTCC development, and reducing dielectric constant and dielectric loss. These advancements will further enhance LTCC materials' suitability for high-performance electronic packaging, addressing the growing demands for miniaturization, reduced weight, and increased reliability in electronic devices.

D. SiCp/Al Matrix Composites and Diamond

New-generation inorganic composite materials have gained significant attention for their outstanding performance. For a lightweight design, SiC particle-reinforced aluminum matrix composites (SiCp/Al) offer high thermal conductivity (100–200 $W\cdot m^{-1}\cdot {}^{\circ}C^{-1}$), adjustable CTE, low density, and excellent strength and hardness, making them valuable in electronic packaging. By varying the SiC volume fraction, the thermal, physical properties, and density of SiCp/Al can be tailored, enabling its use as both a heatsink for power devices and an insulating substrate material [87], [88], [89], [90]. To ensure electrical insulation, techniques such as plasma electrolytic oxidation (PEO) are commonly employed to form a ceramic layer on the surface. This insulating layer not only provides protection but also improves thermal conductivity, opening new avenues for the design and optimization of next-generation integrated power electronic modules [see Fig. 5(a)] [91], [92], [93], [94].

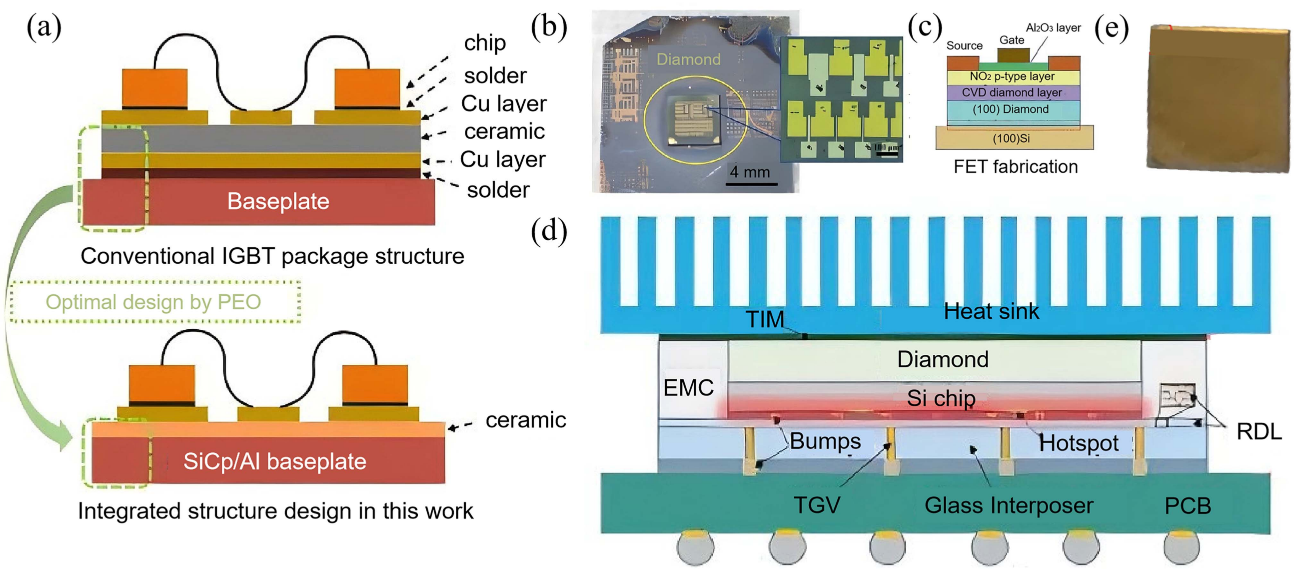

Fig. 5. Devices and products utilizing next-generation inorganic composite substrates. (a) Simplified packaging structure schematic utilizing PEO-coated SiCp/Al. (b) Hydrogen-terminated diamond surface. (c) Diagram illustrating diamond FET fabrication. (d) Schematic structure of diamond-on-chip-on-glass interposer (DoCoG) interposer integration. (e) Image of bonded diamond/Cu sample [87], [95], [96]. Reproduced with permission. Copyright 2017 Elsevier Ltd., copyright 2024 Springer Cham, copyright 2019 AIP Publishing.

Advancements in synthetic diamond technology have significantly reduced the cost of diamond particles. With the high thermal conductivity (2.2×10^3 $W{\cdot}m^{-1}{\cdot}°C^{-1}$), diamond is a highly promising inorganic nonmetallic thermal management material [95]. Techniques such as direct bonding of diamond with semiconductors and direct bonding with metals such as Al and Cu enable the production of low thermal resistance power modules using diamond as the thermal substrate as shown in Fig. 5(b)–(d) [95], [97]. Diamond/copper composites, produced through various processes [see Fig. 5(e)], can achieve thermal conductivities exceeding 500 W/(m·°C). Pressure-free SiC diamond composites can surpass 650 $W{\cdot}m^{-1}{\cdot}°C^{-1}$ in thermal conductivity, and with optimized particle distribution, values can exceed 800 $W{\cdot}m^{-1}{\cdot}°C^{-1}$ [96], [98], [99]. Using these materials will advance the development of higher power and higher performance electronic devices, significantly extending their operational life under equivalent power conditions, particularly in military and aerospace applications with stringent performance and reliability demands. However, most ultrahigh thermal conductivity inorganic composite substrates remain in the experimental phase and require further research and development. Current research efforts focus on increasing composite density, improving interface properties, and refining processing techniques to enable commercial applications.

V. Thermal Interface Materials (TIMs)

The heat dissipation methods for power devices are mainly divided into direct and indirect heat dissipation [100] [see Fig. 6(a)]. The direct heat dissipation method directly exchanges the heat generated by the chip with the external environment through a heat sink. In contrast, the indirect heat dissipation method first transfers the chip's heat to the package shell, then from the shell to the heat sink, and finally exchanges the heat with the external environment. In either method, when in direct contact with the heat sink, surface roughness causes the presence of numerous nano-sized "peaks" and "valleys" on the surface. This results in a limited actual contact area, with the remaining space being filled by air. Since the thermal conductivity of air is only 0.025 $W{\cdot}m^{-1}{\cdot}°C^{-1}$, this increases the interfacial thermal resistance, severely hindering the effective conduction of heat [101]. To address this issue, high thermal conductivity TIMs can be used to eliminate air gaps and establish an effective heat transfer path between the heat source and the heat sink [see Fig. 6(b)]. Ideal thermal interface materials should have high thermal conductivity, low thermal resistance, good wettability, easy installation, and low cost. Currently available thermal interface materials on the market include thermal grease, thermal tapes, thermal pads, thermal oils, metallic solders, and phase change materials.

A. High Thermal Conductivity Fillers

Thermal interface materials such as thermal grease, thermal tapes, and thermal pads are commonly used in electronic devices. Their base materials typically include synthetic resins, such as thermoplastic resins (e.g., polyvinyl alcohol, polyamide) and thermosetting resins (e.g., epoxy resin, phenolic resin, unsaturated polyester). The thermal conductivity of these base materials is relatively low, so to meet the high thermal conductivity demands, high thermal conductivity fillers are usually added. The size and shape of the fillers significantly affect the thermal conductivity of the thermal interface material [102]. The impact of different filler morphologies on the internal heat transport paths of the material is shown in Fig. 6(c). Among the traditional thermal interface material fillers, metal fillers are widely used

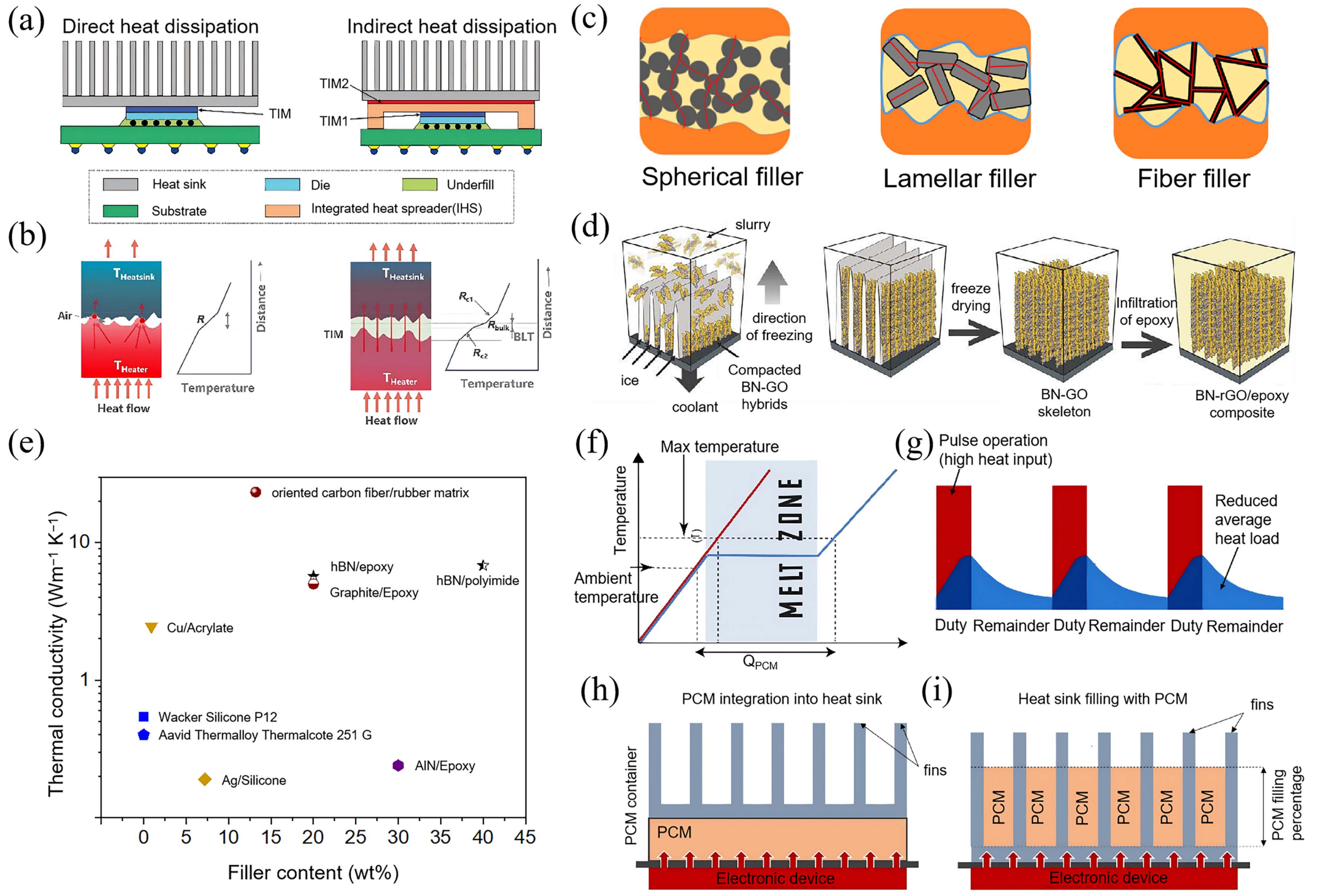

Fig. 6. Application mechanism and methods of TIM materials. (a) Direct and indirect heat dissipation methods for power devices. (b) Schematic diagram of thermal interface materials (right column) that promote heat dissipation. (c) Schematic diagram of thermal conductivity mechanism of fillers with different shapes of thermal interface materials. (d) Schematic diagram of vertical arrangement of two-dimensional material BN in epoxy. (e) Performance comparison of common thermal interface materials (TIMs) and TIMs filled with different materials. (f) Phase change material temperature rise versus time. (g) Role of phase change materials in pulse operation. (h) Schematic diagram of phase change materials as thermal interface materials. (i) Application of phase change materials combined with heat sinks [100], [101], [116], [117], [118]. Reproduced with permission. Copyright 2006, IEEE, copyright 2023 Elsevier Ltd, copyright 2022 Elsevier Ltd.

due to their high thermal conductivity, with common metal materials having thermal conductivities generally above 200 $W{\cdot}m^{-1}{\cdot}°C^{-1}$. However, the thermal expansion coefficient of these metal fillers is difficult to match with that of semiconductor devices, which may lead to incompatibility between materials during temperature changes, thus affecting the stability and lifespan of the device. In addition, metal fillers are generally costly. In high power density power electronic devices, thermal interface materials filled with metals often require composite techniques to optimize the thermal conductivity of metals. These techniques include fiber reinforcement and particle enhancement, aiming to improve the overall thermal conductivity of the material while maintaining compatibility with the thermal expansion coefficient of electronic devices, thereby enhancing the performance and reliability of thermal interface materials [103].

Inorganic nonmetallic fillers, due to their excellent mechanical strength, cost-effectiveness, and high-temperature resistance, have become a key component in the field of thermal interface materials [104]. Specifically, ceramic materials such as aluminum oxide (Al_2O_3), silicon nitride (Si_3N_4), and aluminum nitride (AlN) have shown potential as alternatives to metal fillers due to their good thermal conductivity and electrical insulation properties. Al_2O_3 is favored for its low cost and widespread availability, but its thermal conductivity is relatively low, making it unsuitable for meeting the current industry's cooling performance demands. In contrast, AlN fillers have become a new favorite due to their low dielectric constant and high thermal conductivity (150–300 $W{\cdot}m^{-1}{\cdot}°C^{-1}$). The thermal conductivity of AlN is an order of magnitude higher than that of Al_2O_3, largely due to the lighter atomic mass of nitrogen and the stronger bond energy formed with aluminum atoms [105]. Despite its high thermal conductivity, AlN has the significant drawback of being prone to hydrolysis. On the other hand, Si_3N_4 is regarded as the best overall thermal filler due to its excellent thermal conductivity, outstanding bending strength, and fracture toughness [106]. However, the structural complexity of Si_3N_4 can lead to greater phonon scattering, and impurities, defects, and porosity easily formed during the preparation process can adversely affect the final thermal conductivity of Si_3N_4 [107]. To address these challenges, it is crucial to find novel materials that can solve the limitations in thermal conductivity and high mass density present in traditional thermal interface materials.

Two-dimensional (2-D) nanomaterials, such as graphene, boron nitride (BN), transition metal carbide/nitride, black phosphorus, and molybdenum disulfide, exhibit outstanding anisotropic thermal conductivity due to their lamellar structure, which shows great promise in replacing traditional thermally conductive materials and becoming a novel candidate for next-generation electronics [108]. In micro/nano electronic devices, phonons are the primary carriers of heat in semiconductor materials. Both 2-D graphene and hexagonal BN (hBN) have heat conduction mechanisms based on phonons. Graphene, as the first successfully fabricated 2-D material, has attracted extensive attention since its discovery. In terms of thermal conduction, graphene performs exceptionally well, with its intrinsic thermal conductivity at room temperature reaching 2000–3000 $W \cdot m^{-1} \cdot {}^{\circ}C^{-1}$, making it the highest thermal conductivity material known to date, even surpassing that of diamond [109]. When single-layer or multilayer graphene is mixed with epoxy resin, studies have found that as the graphene doping ratio increases, the thermal conductivity of the mixture also increases. Specifically, samples with a 10% doping volume ratio exhibited a 2300% increase in thermal conductivity compared to pure epoxy resin, reaching about 5.2 $W \cdot m^{-1} \cdot {}^{\circ}C^{-1}$. Additionally, doping experiments in commercial thermal grease showed that doping with only 2% graphene could increase the thermal conductivity from about 5.8 to about 14 $W \cdot m^{-1} \cdot {}^{\circ}C^{-1}$, without significant changes in mechanical properties before and after doping [110]. In addition to the above materials, graphene fibers [111], [112], graphene laminate materials [113], graphene nanofluids [114], and graphene foams [115] are also excellent graphene-based fillers. These materials can meet different needs in various environments.

2-D BN has attracted widespread attention due to its excellent thermal conductivity and outstanding insulating properties. Among various 2-D materials, BN stands out for its high thermal conductivity and smooth surface, making it a highly promising heat dissipation material. This material exhibits significant anisotropic thermal properties, with its thermal conductivity in the planar direction reaching up to 600 $W \cdot m^{-1} \cdot {}^{\circ}C^{-1}$, while its thermal conductivity in the vertical direction is only 30 $W \cdot m^{-1} \cdot {}^{\circ}C^{-1}$. A similar issue is also present in 2-D graphene materials [119]. Therefore, TIMs with higher thermal conductivity in the planar direction can more effectively facilitate heat transfer and address the "hot spot" dissipation problem in electronic devices [120]. By improving the orientation of BN in thermal interface materials, vertical alignment can fully utilize its planar thermal conductivity [116] [see Fig. 6(d)]. Chongqing University prepared a composite material of vertically aligned hexagonal boron nitride and silicone rubber through a roller pressing process. Compared with randomly oriented BN/silicone rubber TIMs, this vertically aligned BN composite material showed a significant increase in longitudinal thermal conductivity, and when the BN content reached 60 wt.%, the longitudinal thermal conductivity of the oriented BN/silicone rubber TIM reached 7.62 $W \cdot m^{-1} \cdot {}^{\circ}C^{-1}$, approximately 36.3 times that of pure silicone rubber [121]. Moreover, one significant advantage of BN is its insulating property, which means it can directly contact electronic devices without the risk of short-circuiting.

Fig. 6(e) summarizes the performance comparison of common TIMs and TIMs filled with different materials [122]. It is evident that inorganic nonmetallic materials, especially advanced 2-D materials, exhibit superior thermal conductivity when used as fillers. Furthermore, the morphology of the filler plays a crucial role in constructing thermal conduction networks within polymers, as illustrated in Fig. 6(c). Compared with traditional spherical fillers, fibrous and sheet-like fillers are more effective in forming complete thermal conduction paths at lower filler concentrations under the same volumetric loading. Therefore, selecting 2-D materials as fillers significantly enhances the thermal conductivity of thermal interface materials. The application of 2-D materials in thermal management primarily focuses on two key directions: horizontal alignment, serving as heat-spreading materials to prevent heat accumulation in devices, and vertical alignment, to enhance thermal transport across interfaces. However, while research on the mass production of 2-D materials is ongoing, several technical challenges must be addressed before their practical application, including further performance improvements, extended service life, and better compatibility with existing technologies [123]. Overcoming these challenges will pave the way for the widespread use of 2-D materials in thermal management.

B. Phase Change Materials (PCMs)

Phase change cooling technology is an important development direction for cooling systems in high-power density power modules [118]. Thermal conductive PCMs, as an innovative example of TIMs, have gained widespread attention in the industry due to their unique phase change capabilities [see Fig. 6(f)]. These materials store thermal energy by the phase change from solid to liquid—the latent heat from melting or freezing is at least 1–2 orders of magnitude higher than the energy stored by specific heat. These materials are particularly suitable for smoothing out thermal energy during pulsed operation, short-term thermal storage when a suitable heatsink is not available, and protection from failure during coolant interruptions when the cooling system is temporarily unavailable [see Fig. 6(g)]. In addition, heat interface materials made from phase change materials can be specifically designed to optimize the thermal exchange between power-dense electronic devices and cooling systems [see Fig. 6(h)]. In the liquid state, PCMs can quickly and evenly transfer heat from the core region of electronic components to the heatsink through their unique structure and carefully optimized heat transfer paths, greatly improving heat transfer efficiency. By constructing low-resistance and efficient thermal conduction channels, the thermal resistance between the electronic device and the heatsink is minimized, thus maximizing the performance of the heatsink [124], [125]. Notably, when the heat source dissipates and the environment stabilizes, thermally conductive PCMs can reverse the phase change from liquid to solid, restoring their original form. This reversible phase change property gives the material the ability to be recycled, reducing the frequency of replacement.

Metals, organic materials, and inorganic nonmetallic materials all have corresponding PCMs systems. Metal and eutectic alloy-based PCMs are characterized by high thermal conductivity and excellent thermal stability, with minimal volume change during phase transitions. However, they exhibit relatively low latent heat of fusion and may interact with container materials at high temperatures in the liquid phase, potentially affecting long-term stability. Additionally, these materials lack electrical insulation properties. Organic phase change materials have high melting enthalpy, small supercooling, and good thermal reliability, with no phase separation issues [118]. However, their flammability and low thermal conductivity limit their application in certain specialized cases. Common examples include paraffin, sugar alcohols, fatty acids, and ethylene glycol. Compared to organic phase change materials, inorganic salt hydrates as phase change materials have higher latent heat of fusion, higher thermal conductivity, negligible volume changes during phase transition, suitable transition temperatures, and lower costs. Inorganic phase change materials mainly include nitrates, carbonates, chlorides, sulfates, fluorides, and their mixtures or eutectics. Inorganic PCMs have a higher heat storage capacity and are more suitable for high-temperature applications [126]. However, phase change materials also have some challenges when used as thermal interface materials, such as low thermal conductivity, supercooling, corrosion, and shape stability. To improve the effective thermal conductivity of composite materials, thermal enhancers, such as graphene and carbon nanotubes, are often added in the preparation of composite materials. These materials are widely used to enhance the thermal conductivity of composites due to their high thermal conductivity and excellent thermal corrosion resistance at medium-to-high working temperatures. Additionally, some studies use matrix foams or ceramic materials to form composites and enhance heat transfer [127], [128]. To achieve better leak resistance in phase change thermal interface materials, researchers have started encapsulating phase change materials in micro/nanocapsules or porous packaging, which are then added to the thermal interface material system. This encapsulation technology not only addresses leakage issues but also increases the specific surface area of the phase change materials, improving their thermal response speed and heat transfer efficiency, thereby enabling more efficient thermal energy storage and temperature control [129].

PCMs have received significant attention due to their excellent transient thermal management potential. An ideal phase change material should possess high energy storage density, low volumetric thermal expansion, stable physical and chemical properties, and high thermal conductivity. The current key direction in technology development is how to further enhance the transient response speed, energy storage density, and long-term stability of phase change materials. At the same time, researchers are actively exploring simple methods to enhance the overall thermal performance of traditional heatsinks, where the coupling of the heatsink surface with phase change materials can combine the high heat capacity of PCMs with the high thermal conductivity of traditional heatsinks (typically made of copper or aluminum), representing a promising optimization area [see Fig. 6(i)] [130], [131]. In the application field of power devices, there are still many gaps in the research on phase change material packaging processes and transient thermal mechanisms. Further studies in these areas will help improve the thermal management efficiency of SiC power modules, making it an important topic for technological progress in this field.

VI. Embedded Packaging Technology

With the widespread application of SiC MOSFETs and other power devices in industries like electric vehicles, the demand for miniaturization and high integration in power electronic systems has intensified [132], [133]. At the 2023 PCIM conference, Infineon and Schweizer Electronic AG showcased 1200 V CoolSiC embedded PCB technology, which garnered significant industry attention toward the concept of embedded packaging [see Fig. 7(a)] [134], [135], [136], [137]. Embedded packaging integrates power chips into the substrate through processes such as encapsulation and lamination, utilizing redistribution layer (RDL) technology to create circuit patterns for electrical connections, as illustrated in Fig. 7(a). This packaging method not only reduces device package size and increases integration but also shortens electrical interconnect paths, thereby minimizing parasitic parameters [138]. Furthermore, embedded packaging structures enable platforms for 3-D stacked integration and double-sided cooling, offering superior electrical performance and thermal management capabilities [132], [139], [140]. Research on new integrated packaging technologies for power electronics, including 3-D packaging, hybrid packaging, and press-fit packaging, can all fall under the scope of embedded packaging [141], [142], [143], [144].

A. PCB Embedded Packaging

PCB embedded packaging is a cost-effective and compact microelectronic packaging technology with significant potential [145], [146]. The Fraunhofer Institute for Applied Solid State Physics has developed a PCB-embedded GaN-on-Si half-bridge power module that integrates GaN chips with gate drivers into PCB substrates, along with temperature and current sensors [147]. Researchers from Delft University of Technology compared the thermal resistance of PCB-embedded packaging and mainstream wire-bond packaging for SiC power devices, finding that embedded packaging with double-sided cooling exhibited lower thermal resistance than single-sided cooling wire-bond packaging [148], [149], [150]. While PCBs, consisting of organic insulation layers and metal circuit layers, are cost-effective and easy to machine—making them the most common packaging substrate material—the poor thermal performance of organic materials leads to a relatively low composite thermal conductivity for PCB substrates (0.2–0.3 $W\cdot m^{-1}\cdot {}^{\circ}C^{-1}$), with extreme cases potentially resulting in carbonization [151]. Consequently, traditional PCB substrates face limitations in meeting the thermal management requirements of power device packaging.

B. Ceramic Substrate Embedded Packaging

Traditional ceramic-embedded power modules typically involve embedding power chips into a ceramic framework that is

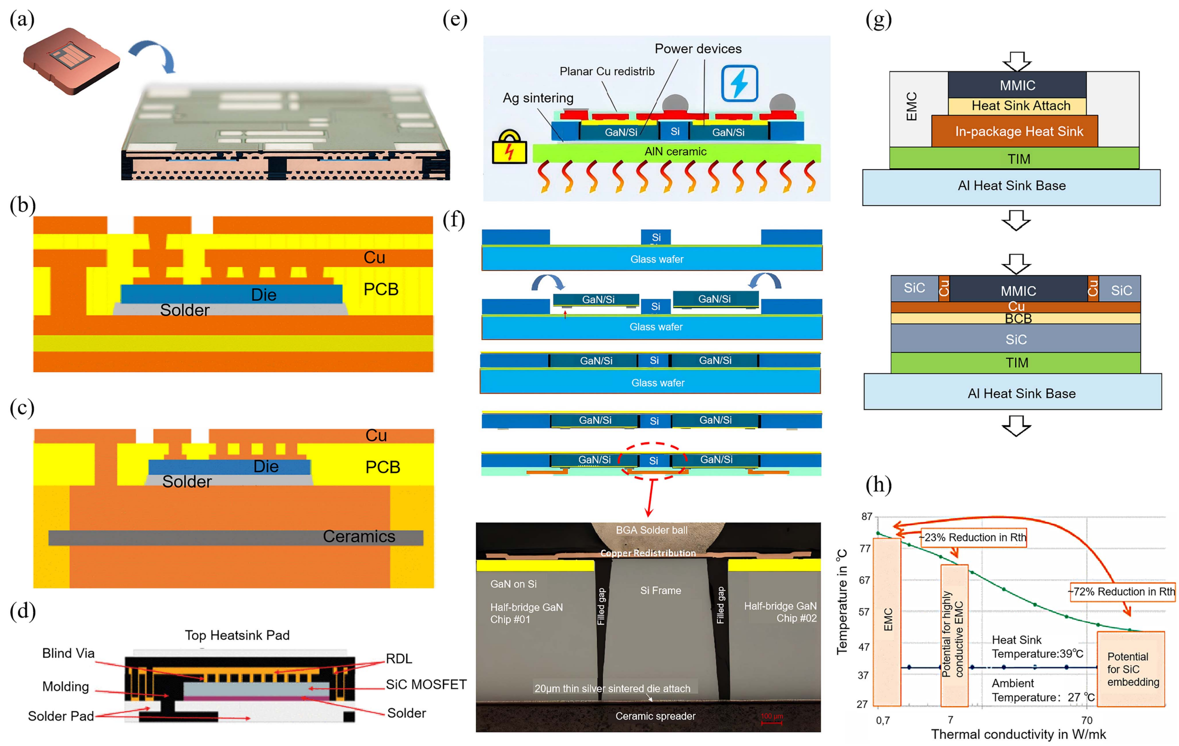

Fig. 7. Schematic diagram of different embedded packaging structures. (a) 1200 V CoolSiC™ Gen2p chips into the PCB. (b) Schematic diagram of embedded PCB packaging structure. (c) Schematic diagram of embedded PCB packaging structure with ceramic substrate. (d) Schematic diagram of fan-out panel-level packaging SiC MOSFET. (e) Schematic diagram of fan-out wafer-level packaging GaN/Si with Si interposer. (f) Wafer level process flow of fan-out wafer-level packaging GaN/Si with Si interposer. (g) Schematic diagram of embedded SiC packaging structure and comparison with traditional structure. (h) Simulation of thermal resistance using the same fan-out embedded structure but different materials.[156], [158], [159], [163] Reproduced with permission. Copyright 2017 Elsevier Ltd., copyright 2024 Springer Cham, copyright 2019 AIP Publishing.

covered by a dielectric layer featuring via holes on the Al pads of the chips [152]. Ceramic substrates can also be combined with PCB, with the basic structure shown in Fig. 7(c). To meet the increasing power density demands of power devices, the integration of ceramic substrates has become particularly critical. Ceramic substrates can include silicon nitride (Si_3N_4)-based AMB, DBC, or DPC substrates (see Table III). These inorganic nonmetallic substrates provide excellent electrical insulation and high thermal conductivity. Researchers at the University of Cambridge proposed a standard cell structure composed of an AMB substrate and a flexible printed circuit board. This structure offers high thermal conductivity, complete electrical insulation, and low stray inductance, enhancing the performance of SiC MOSFET devices [77], [136]. However, challenges remain in integrating ceramic materials with traditional process flows. To address this, ceramic substrates should be as compact as possible and closely match the size of power chips. Notably, LTCC combined with fuzz button technology can replace traditional interconnections between DBC substrates and wire bonds. Moreover, LTCC itself can serve as an embedded packaging technology, allowing features such as cavity openings [153], [154].

C. Fan-Out Packaging

Fan-out packaging is a critical technology for device miniaturization and a significant component of embedded packaging. In this method, the RDL is crucial for electrical connections and is typically realized through an EMC molding process combined with drilling [155]. Fudan University has developed a 1200 V/136 A fan-out panel-level packaging SiC MOSFET with dimensions of $8 \times 8 \times 0.75$ mm, featuring low parasitic inductance and low thermal resistance [156] [as shown in Fig. 7(d)]. However, the low thermal conductivity of EMC and the multiple molding processes involved can impact device reliability. Combining embedded structures with fan-out packaging can further enhance device performance. With advancements in through-silicon via technology, silicon interposers are increasingly being used in power systems [157]. Fraunhofer IZM has developed a fan-out wafer-level embedding technology capable of creating highly compact half-bridge modules based on planar GaN semiconductor devices [see Fig. 7(e)]. This technology supports the integration of ceramic spreaders, forming a BGA-like GaN half-bridge package with dimensions of $12 \times 9 \times 1.2$ mm and a thermal resistance as low as 0.4 K/W, suitable for high-voltage applications up to 2.5 kV, with the wafer level process flow shown in Fig. 7(f) [158]. Nonetheless, silicon, as a semiconductor material, exhibits relatively poor breakdown strength. This issue can be addressed through additional insulation techniques, although this often leads to higher costs. Insufficient rigidity in thin layers can also compromise mechanical performance. As SiC wafer manufacturing technologies advance, including reduced defect densities and increased wafer diameters, mature silicon-based technologies can be adapted for SiC. SiC offers higher thermal conductivity, superior mechanical properties, and greater chemical stability. Fraunhofer IZM has also developed a SiC-based fan-out packaging process for high-power applications, which is compared with traditional structures as shown in Fig. 7(g) [159], [160], [161], [162]. FEM simulations show that this packaging form can reduce thermal resistance by 72% [as illustrated in Fig. 7(h)]. However, due to SiC's high chemical stability, conventional processes for silicon substrate through-vias are often unsuitable for SiC structuring. Moreover, SiC wafer packaging is typically aimed at harsher environments, requiring innovative packaging technologies and materials to overcome challenges, such as insulation methods distinct from those used for silicon substrates.

Modular and intelligent packaging of power devices significantly enhances manufacturability and reliability while reducing packaging and application costs. The application of advanced packaging technologies such as fan-out packaging in power devices poses new challenges to traditional manufacturing processes and packaging materials. In this context, various inorganic non-metallic wafer substrates play a more critical role. However, whether silicon-based or SiC-based substrates, issues such as poor insulation performance, high manufacturing costs, and small wafer substrate sizes remain obstacles, limiting their suitability for large-scale production. In contrast, glass substrates seem to offer a better alternative. Glass substrates hold significant promise for power module packaging [164], [165]. Glass substrates offer high resistivity, high modulus, low dielectric loss, minimal warpage (less than 30 μm for 8-in substrates), low thermal deformation, adjustable dielectric constant and CTE, as well as exceptional thickness variation (TTV, < 0.5 μm) and flatness ($\pm$ 2.5 μm). They can also be produced in large sizes (100×100–650×650 mm) with smooth surfaces (RMS, < 1 nm) and easy processing, garnering attention in semiconductor heterogeneous integration packaging. Major semiconductor manufacturers such as Intel, Nvidia, and Samsung are expected to launch glass substrate-based products soon. Glass substrate manufacturers such as Corning, Schott, NEG, and AGC have introduced various high-performance glass substrates for global chipmakers and integrated device manufacturers. Given the potential of glass substrates for device scaling, research institutions such as The Georgia Institute of Technology, The University of Tokyo, and National Tsing Hua University demonstrated proof-of-concept results, including micron-scale laser vias, sub-micron RDL wiring, and fan-out level packaging based on glass substrates [53], [166], [167], [168]. Glass substrates can enable higher chip density and integration of passive components such as multilayer ceramic capacitors, advancing power modules toward greater performance and power density. However, further innovation is required for glass substrate-based packaging solutions, and researchers are actively exploring new approaches.

VII. Conclusion

With the continuous improvement in the performance and operating temperature of power chips, as well as the maturity of high-frequency, high-temperature WBG power chip products, the market demand is growing, making the exploration of high-performance packaging materials increasingly urgent. This article provides a detailed review of the application of inorganic nonmetallic materials in power electronics packaging, covering components such as encapsulants, substrate materials, TIMs, and embedded packaging technologies, and the following conclusions are drawn.

1) Cement and glass materials exhibit excellent high-temperature and insulating properties, designed for specialized environments, including high temperatures, high voltages, radiation, and corrosion. However, as new encapsulants, their processing flows differ from those of traditional polymer-based encapsulants and cannot be adapted to existing packaging equipment. Future developments will focus on reducing production costs and optimizing process flows.
2) Inorganic nonmetallic materials play a crucial role in traditional substrate materials. Multilayer ceramic technologies (including HTCC and LTCC) offer excellent integration capabilities, providing constructive solutions for multichip power packaging and heterogeneous integration of power electronics. However, the high cost remains a key limiting factor for the development of this technology. New-generation inorganic composite substrates, such as SiCp/Al matrix composites and diamond, are progressing toward commercialization.
3) The performance of TIMs largely depends on the fillers used. Inorganic nonmetallic fillers, particularly new 2-D materials like graphene and hBN, can further enhance the heat dissipation capabilities of TIMs. PCMs, a type of TIM, have attracted attention for their excellent transient thermal management potential. Inorganic nonmetallic PCMs, with higher thermal conductivity and smaller volume changes, make them more suitable for power devices.
4) Miniaturization, low cost, and high reliability are the relentless pursuit of large-power semiconductor device users, making embedded packaging a focal point in the power semiconductor industry. Fan-out packaging technology is a key technology for achieving miniaturized embedded devices and large-scale low-cost production, where inorganic nonmetallic material substrates (such as Si wafers, SiC wafers, or future glass wafers) play a critical role.

All inorganic nonmetallic packaging materials reviewed exhibit more significant advantages in electrical, thermal, and mechanical aspects. Nevertheless, organic packaging materials still dominate certain power device components due to their flexibility, ease of implementation, maturity, and lower cost. However, with the growing demand from high-end users in sectors such as electric vehicles, renewable energy generation, and multielectric aircraft, new packaging structures, advanced packaging technologies, and material applications based on inorganic nonmetallic materials will continue to emerge.

References

[1] J. R. Dietz, B. Jiang, A. M. Day, S. A. Bhave, and E. L. Hu, "Spin-acoustic control of silicon vacancies in 4H silicon carbide," *Nat. Electron.*, vol. 6, no. 10, pp. 739–745, Oct. 2023, doi: 10.1038/s41928-023-01029-4.

[2] Y. Li et al., "State-of-the-art medium- and high-voltage silicon carbide power modules, challenges and mitigation techniques: A review," *IEEE Trans. Compon., Packag., Manuf. Technol.*, vol. 14, no. 12, pp. 2177–2195, Dec. 2024, doi: 10.1109/TCPMT.2024.3391653.

[3] X. Lu, L. Wang, Q. Yang, F. Yang, Y. Gan, and H. Zhang, "Investigation and comparison of temperature-sensitive electrical parameters of SiC MOSFET at extremely high temperatures," *IEEE Trans. Power Electron.*, vol. 38, no. 8, pp. 9660–9672, Aug. 2023, doi: 10.1109/TPEL.2023.3267472.

[4] Q. Zhang and P. Zhang, "A junction temperature and package aging decoupling evaluating method for SiC MOSFETs based on the turn-on drain-source current overshoot," *IEEE Trans. Power Electron.*, vol. 38, no. 11, pp. 14537–14546, Nov. 2023, doi: 10.1109/TPEL.2023.3307241.

[5] X. Zhong, X. Wu, W. Zhou, and K. Sheng, "An all-SiC high-frequency boost DC–DC converter operating at 320 °C junction temperature," *IEEE Trans. Power Electron.*, vol. 29, no. 10, pp. 5091–5096, Oct. 2014, doi: 10.1109/TPEL.2014.2311800.

[6] F. Yang et al., "Compact-interleaved packaging method of power module with dynamic characterization of 4H-SiC MOSFET and development of power electronic converter at extremely high junction temperature," *IEEE Trans. Power Electron.*, vol. 38, no. 1, pp. 417–434, Jan. 2023, doi: 10.1109/TPEL.2022.3198835.

[7] S. Graham and S. Choi, "Integrating boron arsenide into power devices," *Nat. Electron.*, vol. 4, no. 6, pp. 380–381, 2021, doi: 10.1038/s41928-021-00604-x.

[8] N. Pavlicek et al., "Patterning and CTE-matching of contacts to optimize thermomechanical stress in power semiconductor pre-packages," in *Proc. 12th Int. Conf. Integr. Power Electron. Syst.*, 2022, pp. 1–7.

[9] G. Li et al., "Integrated microthermoelectric coolers with rapid response time and high device reliability," *Nat. Electron.*, vol. 1, no. 10, pp. 555–561, 2018, doi: 10.1038/s41928-018-0148-3.

[10] C. Papadopoulos, C. Corvasce, A. Kopta, D. Schneider, G. Pâques, and M. Rahimo, "The influence of humidity on the high voltage blocking reliability of power IGBT modules and means of protection," *Microelectron. Rel.*, vol. 88–90, pp. 470–475, 2018, doi: 10.1016/j.microrel.2018.07.130.

[11] T. Baba et al., "Radiation-induced degradation of silicon carbide MOSFETs – A review," *Mater. Sci. Eng., B*, vol. 300, 2024, Art. no. 117096, doi: 10.1016/j.mseb.2023.117096.

[12] R. Luo, Y. Duan, B. Sun, J. Q. Zhang, J. Fan, and P. Liu, "Total ionizing effects on static characteristics of 1200V SiC MOSFET power devices with planar and trench structures," in *Proc. 20th China Int. Forum Solid State Lighting 9th Int. Forum Wide Bandgap Semicond.*, 2023, pp. 88–91, doi: 10.1109/SSLChinaIFWS60785.2023.10399707.

[13] N. Murayama, K. Hirao, M. Sando, T. Tsuchiya, and H. Yamaguchi, "High-temperature electro-ceramics and their application to SiC power modules," *Ceram. Int.*, vol. 44, no. 4, pp. 3523–3530, 2018, doi: 10.1016/j.ceramint.2017.11.140.

[14] J. Reimers, L. Dorn-Gomba, C. Mak, and A. Emadi, "Automotive traction inverters: Current status and future trends," *IEEE Trans. Veh. Technol.*, vol. 68, no. 4, pp. 3337–3350, Apr. 2019, doi: 10.1109/TVT.2019.2897899.

[15] H. Zhang et al., "Progress of ultra-wide bandgap Ga_2O_3 semiconductor materials in power MOSFETs," *IEEE Trans. Power Electron.*, vol. 35, no. 5, pp. 5157–5179, May 2020, doi: 10.1109/TPEL.2019.2946367.

[16] Y. Wang, Y. Wu, S. Jones, X. Dai, and G. Liu, "Challenges and trends of high power IGBT module packaging," in *Proc. IEEE Conf. Expo Transp. Electrific. Asia-Pacific*, 2014, pp. 1–7, doi: 10.1109/ITEC-AP.2014.6940851.

[17] Y. Qin et al., "Thermal management and packaging of wide and ultra-wide bandgap power devices: A review and perspective," *J. Phys. D, Appl. Phys.*, vol. 56, no. 9, 2023, Art. no. 093001, doi: 10.1088/1361-6463/acb4ff.

[18] Y. Yan et al., "A novel double-sided cooling silicon carbide power module with ultra-low parasitic inductance based on an interleaved power loop," *IEEE Trans. Power Electron.*, vol. 39, no. 10, pp. 12570–12588, Oct. 2024, doi: 10.1109/TPEL.2024.3410509.

[19] Y. Zhang et al., "Comprehensive analysis and optimization of parasitic capacitance on conducted EMI and switching losses in hybrid-packaged SiC power modules," *IEEE Trans. Power Electron.*, vol. 38, no. 11, pp. 13988–14003, Nov. 2023, doi: 10.1109/TPEL.2023.3306892.

[20] Y. Yan, C. Chen, Z. Wu, J. Guan, J. Lv, and Y. Kang, "A high power density double-side-end double-sided bonding SiC half-bridge power module," *IEEE Trans. Transp. Electrific.*, vol. 9, no. 2, pp. 3149–3163, Jun. 2023, doi: 10.1109/TTE.2022.3225115.

[21] P. Beckedahl, I. Bogen, and J. Steger, "SiC automotive power module with laser welded, ultra low inductive terminals and up to 900Arms phase current," in *Proc. 12th Int. Conf. Integr. Power Electron. Syst.*, 2022, pp. 1–5.

[22] F. Hou et al., "Review of die-attach materials for SiC high temperature packaging," *IEEE Trans. Power Electron.*, vol. 39, no. 10, pp. 13471–13486, Oct. 2024, doi: 10.1109/TPEL.2024.3417529.

[23] L. Wang, W. Wang, R. J. E. Hueting, G. Rietveld, and J. A. Ferreira, "Review of topside interconnections for wide bandgap power semiconductor packaging," *IEEE Trans. Power Electron.*, vol. 38, no. 1, pp. 472–490, Jan. 2023, doi: 10.1109/TPEL.2022.3200469.

[24] D. Lu, X. Wang, H. Pan, X. Zheng, M. Li, and H. Ji, "Low-temperature direct bonding of sputtered nanocrystalline Ag film for power electronic packaging: Bonding mechanism, thermal characteristics, and reliability," *IEEE Trans. Power Electron.*, vol. 39, no. 5, pp. 6040–6051, May 2024, doi: 10.1109/TPEL.2024.3368666.

[25] L. A. Navarro et al., "Thermomechanical assessment of die-attach materials for wide bandgap semiconductor devices and harsh environment applications," *IEEE Trans. Power Electron.*, vol. 29, no. 5, pp. 2261–2271, May 2014, doi: 10.1109/TPEL.2013.2279607.

[26] W. Mu, A. Janabi, B. Hu, L. Shillaber, and T. Long, "Liquid metal fluidic connection and floating die structure for ultralow thermomechanical stress of SiC power electronics packaging," *IEEE Trans. Power Electron.*, vol. 39, no. 7, pp. 7808–7814, Jul. 2024, doi: 10.1109/TPEL.2024.3379121.

[27] E. Gurpinar, S. Chowdhury, B. Ozpineci, and W. Fan, "Graphite-embedded high-performance insulated metal substrate for wide-bandgap power modules," *IEEE Trans. Power Electron.*, vol. 36, no. 1, pp. 114–128, Jan. 2021, doi: 10.1109/TPEL.2020.3001528.

[28] J. Chen, A. Li, C. Zhong, L. Zhang, K. Lu, and H. Zeng, "Regulating the valence state of lead ions in lead aluminosilicate glass to improve the passivation performance for advanced chip packaging," *Appl. Surf. Sci.*, vol. 651, 2024, Art. no. 159208, doi: 10.1016/j.apsusc.2023.159208.

[29] J. Chen, W. Chen, L. Zhang, X. Yan, J. Fan, and H. Zeng, "Tuning the thermal and insulation properties of bismuth borate glass for SiC power electronics packaging," *J. Amer. Ceram. Soc.*, vol. 107, no. 4, pp. 2207–2216, 2024, doi: 10.1111/jace.19579.

[30] B. Grummel, R. McClure, Z. Lei, A. P. Gordon, L. Chow, and Z. J. Shen, "Design consideration of high temperature SiC power modules," in *Proc. 34th Annu. Conf. IEEE Ind. Electron.*, 2008, pp. 2861–2866, doi: 10.1109/IECON.2008.4758413.

[31] P. Beckedahl, J. Rudzki, and M. Spang, "Trends in power module packaging and impact of wide bandgap semiconductors," in *Proc. Compon. Power Electron. Their Appl.; ETG Symp.*, 2023, pp. 47–54.

[32] N. Fujishima, "Technical trends of SiC power semiconductor devices and their applications in power electronics," *IEEJ J. Ind. Appl.*, vol. 13, no. 4, pp. 372–378, 2024, doi: 10.1541/ieejjia.23005497.

[33] P. Beckedahl, S. Buetow, A. Maul, M. Roeblitz, and M. Spang, "400 A, 1200 V SiC power module with 1nH commutation inductance," in *Proc. 9th Int. Conf. Integr. Power Electron. Syst.*, 2016, pp. 1–6.

[34] A. I. Emon, H. Mustafeez ul, A. B. Mirza, J. Kaplun, S. S. Vala, and F. Luo, "A review of high-speed GaN power modules: State of the art, challenges, and solutions," *IEEE J. Emerg. Sel. Topics Power Electron.*, vol. 11, no. 3, pp. 2707–2729, Jun. 2023, doi: 10.1109/JESTPE.2022.3232265.

[35] X. Tian et al., "PCB-on-DBC GaN power module design with high-density integration and double-sided cooling," *IEEE Trans. Power Electron.*, vol. 39, no. 1, pp. 507–516, Jan. 2024, doi: 10.1109/TPEL.2023.3311440.

[36] Y. Sun et al., "Packaging a 100kW all-GaN-based three-level active neutral point clamped power module for electric vehicle motor drives," in *Proc. IEEE Energy Convers. Congr. Expo.*, 2023, pp. 5474–5479, doi: 10.1109/ECCE53617.2023.10362757.

[37] R. Paul, A. Hassan, and H. A. Mantooth, "A double-sided cooled power module with embedded decoupling capacitors," *IEEE J. Emerg. Sel. Topics Power Electron.*, vol. 12, no. 2, pp. 1813–1821, Apr. 2024, doi: 10.1109/JESTPE.2023.3348696.

[38] A. I. Emon, Y. Wu, Y. Li, A. B. Mirza, S. Deng, and F. Luo, "A double-sided cooled split-phase SiC power module with fuzz button interposer," *IEEE J. Emerg. Sel. Topics Power Electron.*, vol. 11, no. 5, pp. 4918–4928, Oct. 2023, doi: 10.1109/JESTPE.2023.3294932.

[39] H. Chen et al., "Fabrication and experimental validation of low inductance SiC power module with integrated microchannel cooler," in *Proc. IEEE Appl. Power Electron. Conf. Expo.*, 2023, pp. 366–371, doi: 10.1109/APEC43580.2023.10131620.

[40] D. Ma et al., "A highly integrated Multichip SiC MOSFET power module with optimized electrical and thermal performances," *IEEE J. Emerg. Sel. Topics Power Electron.*, vol. 11, no. 2, pp. 1722–1736, Apr. 2023, doi: 10.1109/JESTPE.2022.3210440.

[41] Y. Park, S. Chakraborty, and A. Khaligh, "Characterization of a bare-die SiC-based, wirebond-less, integrated half-bridge with multi-functional bus-bars," *IEEE Trans. Transp. Electrific.*, vol. 8, no. 3, pp. 3946–3959, Sep. 2022, doi: 10.1109/TTE.2022.3155737.

[42] X. Lyu, X. Tian, H. Li, H. You, and J. Wang, "Design of a lightweight low inductance power module with ceramic baseplates," in *Proc. IEEE Appl. Power Electron. Conf. Expo.*, 2020, pp. 2782–2787, doi: 10.1109/APEC39645.2020.9124073.

[43] C. Marczok, E. Hoene, T. Thomas, A. Meyer, and K. Schmidt, "Low inductive SiC mold module with direct cooling," in *Proc. PCIM Europe; Int. Exhib. Conf. Power Electron., Intell. Motion, Renewable Energy Manage.*, 2019, pp. 1–6.

[44] G. Watt, A. Romero, R. Burgos, and M. Jaksic, "Design of a compact, low inductance 1200 V, 6.5 mΩ SiC half-bridge power module with flexible PCB gate loop connection," in *Proc. IEEE Appl. Power Electron. Conf. Expo.*, 2019, pp. 2786–2793, doi: 10.1109/APEC.2019.8722138.

[45] Z. Huang, C. Chen, Y. Xie, Y. Yan, Y. Kang, and F. Luo, "A high-performance embedded SiC power module based on a DBC-stacked hybrid packaging structure," *IEEE J. Emerg. Sel. Topics Power Electron.*, vol. 8, no. 1, pp. 351–366, Mar. 2020, doi: 10.1109/JESTPE.2019.2943635.

[46] C. Chen, Z. Huang, L. Chen, Y. Tan, Y. Kang, and F. Luo, "Flexible PCB-based 3-D integrated SiC half-bridge power module with three-sided cooling using ultralow inductive hybrid packaging structure," *IEEE Trans. Power Electron.*, vol. 34, no. 6, pp. 5579–5593, Jun. 2019, doi: 10.1109/TPEL.2018.2866404.

[47] S. Behrendt, "Investigation of inorganic encapsulated power modules with enhanced cooling possibilities," in *Proc. IEEE 9th Electron. Syst.-Integration Technol. Conf.*, 2022, pp. 446–451, doi: 10.1109/ESTC55720.2022.9939500.

[48] A. Calmels et al., "First Aerospace-qualified baseless SiC power module Family improves high reliability systems efficiency," in *Proc. PCIM Europe; Int. Exhib. Conf. Power Electron., Intell. Motion, Renewable Energy Manage.*, 2022, pp. 1–10, doi: 10.30420/565822142.

[49] X. Li et al., "Polymer-based electronic packaging molding compounds, specifically thermal performance improvement: An overview," *ACS Appl. Polym. Mater.*, vol. 6, no. 24, pp. 14948–14969, Dec. 2024, doi: 10.1021/acsapm.4c03086.

[50] B. Lyon and C. DiMarino, "Investigation and evaluation of high-temperature encapsulation materials for power module applications," *J. Microelectron. Electron. Packag.*, vol. 20, no. 3, pp. 89–94, 2023.

[51] M. L. Locatelli et al., "Evaluation of encapsulation materials for high-temperature power device packaging," *IEEE Trans. Power Electron.*, vol. 29, no. 5, pp. 2281–2288, May 2014, doi: 10.1109/TPEL.2013.2279997.

[52] R. Khazaka, L. Mendizabal, D. Henry, and R. Hanna, "Survey of high-temperature reliability of power electronics packaging components," *IEEE Trans. Power Electron.*, vol. 30, no. 5, pp. 2456–2464, May 2015, doi: 10.1109/TPEL.2014.2357836.

[53] T. Wang et al., "A novel FOPLP structure with chip first & RDL first process for automotive chip application," in *Proc. IEEE 74th Electron. Compon. Technol. Conf.*, 2024, pp. 1868–1871, doi: 10.1109/ECTC51529.2024.00313.

[54] Q. Zou, G. Xie, G. Lei, Q. Ding, and W. Zhan, "Development and characterization of epoxy molding compound with high glass transition temperature," in *Proc. 23rd Int. Conf. Electron. Packag. Technol.*, 2022, pp. 1–6, doi: 10.1109/ICEPT56209.2022.9873223.

[55] B. Zhang, M. Ghassemi, and Y. Zhang, "Insulation materials and systems for power electronics modules: A review identifying challenges and future research needs," *IEEE Trans. Dielect. Elect. Insul.*, vol. 28, no. 1, pp. 290–302, Feb. 2021, doi: 10.1109/TDEI.2020.009041.

[56] Q. Wang, X. Chen, A. Paramane, J. Li, X. Huang, and N. Ren, "Design of interfacial electrical tree-resistant packaging insulation using grafted silicone elastomer nanocomposites for high-temperature power modules," *IEEE Trans. Power Electron.*, vol. 39, no. 5, pp. 4933–4946, May 2024, doi: 10.1109/TPEL.2024.3365304.

[57] H. Gao and P. Liu, "High-temperature encapsulation materials for power modules: Technology and future development trends," *IEEE Trans. Compon., Packag. Manuf. Technol.*, vol. 12, no. 11, pp. 1867–1881, Nov. 2022, doi: 10.1109/TCPMT.2022.3225960.

[58] J. D. Scofield, J. N. Merrett, J. Richmond, A. Agarwal, and S. Leslie, "Performance and reliability characteristics of 1200 V, 100 A, 200 °C half-bridge SiC MOSFET-JBS diode power modules," in *Proc. Additional Conf. (Device Packag., HiTEC, HiTEN, CICMT)*, 2010, vol. 2010, pp. 000289–000296, doi: 10.4071/HITEC-JScofield-WP22.

[59] S. Kaessner et al., "Novel cement-ceramic encapsulation material for electronic packaging," in *J. Ceram. Sci. Technol.*, vol. 9, no. 4, 2018, doi: 10.4416/JCST2018-00024.

[60] S. Kaessner, M. G. Scheibel, S. Behrendt, B. Boettge, C. Berthold, and K. G. Nickel, "Reliability of novel ceramic encapsulation materials for electronic packaging," *J. Microelectron. Electron. Packag.*, vol. 15, no. 3, pp. 132–139, 2018, doi: 10.4071/imaps.661015.

[61] H. Gao et al., "Finite element modeling for thermal conductivity of cement-based encapsulation materials," in *Proc. 23rd Int. Conf. Electron. Packag. Technol.*, 2022, pp. 1–5, doi: 10.1109/ICEPT56209.2022.9873392.

[62] F. Naumann, B. Boettge, S. Behrendt, R. Eisele, and S. Klengel, "Numerical material design for reliable power electronics with cement-based encapsulation," in *Proc. CIPS; 11th Int. Conf. Integr. Power Electron. Syst.*, 2020, pp. 1–6.

[63] S. Behrendt, R. Eisele, M. G. Scheibel, and S. Kaessner, "Implementation of a new thermal path within the structure of inorganic encapsulated power modules," *Microelectron. Rel.*, vol. 100/101, 2019, Art. no. 113430, doi: 10.1016/j.microrel.2019.113430.

[64] L. Liu, D. Nam, B. Guo, J. Ewanchuk, R. Burgos, and G. Q. Lu, "Glass for encapsulating high-temperature power modules," *IEEE J. Emerg. Sel. Topics Power Electron.*, vol. 9, no. 3, pp. 3725–3734, Jun. 2021, doi: 10.1109/JESTPE.2020.3004021.

[65] L. Liu et al., "Evaluation of a lead glass for encapsulating high-temperature power modules for aerospace application," in *Proc. Int. Electron. Packag. Tech. Conf. Exhib., Amer. Soc. Mech. Engineers*, vol. 59322, 2019, Art. no. V001T06A006, doi: 10.1115/IPACK2019-6393.

[66] Z. Zhang et al., "Package design and analysis of a 20-kV double-sided silicon carbide diode module with polymer nanocomposite field-grading coating," *IEEE Trans. Compon., Packag. Manuf. Technol.*, vol. 14, no. 5, pp. 776–783, May 2024, doi: 10.1109/TCPMT.2024.3381090.

[67] J. Chen et al., "Glass-based encapsulant enabling SiC power devices to long-term operate at 300 °C," *Appl. Surf. Sci.*, vol. 680, 2025, Art. no. 161452, doi: 10.1016/j.apsusc.2024.161452.

[68] B. Kanagaraj, N. Anand, A. Diana Andrushia, and M. Z. Naser, "Recent developments of radiation shielding concrete in nuclear and radioactive waste storage facilities – A state of the art review," *Construction Building Mater.*, vol. 404, 2023, Art. no. 133260, doi: 10.1016/j.conbuildmat.2023.133260.

[69] M. I. Sayyed and G. Lakshminarayana, "Structural, thermal, optical features and shielding parameters investigations of optical glasses for gamma radiation shielding and defense applications," *J. Non-Crystalline Solids*, vol. 487, pp. 53–59, 2018, doi: 10.1016/j.jnoncrysol.2018.02.014.

[70] P. Adhikari and M. Ghassemi, "A comprehensive review of mitigation strategies to address insulation challenges within high voltage, high power density (U)WBG power module packages," *IEEE Trans. Dielect. Elect. Insul.*, vol. 31, no. 5, pp. 2676–2700, Oct. 2024, doi: 10.1109/TDEI.2024.3382070.

[71] Z. Zhang et al., "Insulation capability at 10 kV, >300 V/ns of a nonlinear resistive polymer nanocomposite field-grading coating in a 15-kV silicon carbide module," *IEEE Trans. Power Electron.*, vol. 39, no. 12, pp. 15748–15756, Dec. 2024, doi: 10.1109/TPEL.2024.3445328.

[72] Z. Zhang, Q. Yuchi, C. Nicholas, K. D. T. Ngo, and G. Q. Lu, "Effective field grading at 200 °C of a nonlinear resistive polymer nanocomposite coating for medium-voltage power modules," *IEEE Trans. Power Electron.*, vol. 39, no. 4, pp. 3974–3978, Apr. 2024, doi: 10.1109/TPEL.2024.3351557.

[73] S. Ziesche, C. Lenz, A. Mueller-Koehn, U. Scheithauer, and U. Partsch, "3D Multilayered ceramics – harsh environment interposer technologies expand into 3rd dimension," in *Proc. 7th Electron. Syst. Integration Technol. Conf.*, 2018, pp. 1–5, doi: 10.1109/ESTC.2018.8546387.

[74] B. Liu et al., "A high-reliability SiC-based power module with high-temperature co-fired ceramic interposer for high-temperature applications," in *Proc. IEEE Appl. Power Electron. Conf. Expo.*, 2024, pp. 2551–2555, doi: 10.1109/APEC48139.2024.10509025.

[75] D. Y. Jung et al., "Multi-layer ceramic based surface mount device packaging for 1200 V and 1700 V SiC SBD power semiconductors," in *Proc. IEEE Int. Conf. Consum. Electron. - Asia*, 2020, pp. 1–4, doi: 10.1109/ICCE-Asia49877.2020.9276963.

[76] D. Y. Jung et al., "Switching and heat-dissipation performance analysis of an LTCC-based leadless surface mount package using a power factor correction converter," in *Proc. Int. Conf. Electron., Inf., Commun.*, 2021, pp. 1–3, doi: 10.1109/ICEIC51217.2021.9369757.

[77] P. Sun, X. Cui, S. Huang, P. Lai, Z. Zhao, and Z. Chen, "LTCC based current sensor for silicon carbide power module integration," *IEEE Trans. Power Electron.*, vol. 37, no. 2, pp. 1605–1614, Feb. 2022, doi: 10.1109/TPEL.2021.3104284.

[78] H. G. Jang, D. Y. Jung, D. Cho, K. S. Park, J. W. Lim, and Y. H. Lee, "Power conversion module using LTCC substrate interconnected to power inductor with low DCR," in *Proc. IEEE 8th Electron. Syst.-Integration Technol. Conf.*, 2020, pp. 1–5, doi: 10.1109/ESTC48849.2020.9229808.

[79] B. Bayer et al., "LTCC embedding of SiC power devices for high temperature applications over 400°C," in *Proc. IEEE 8th Electron. Syst.-Integration Technol. Conf.*, 2020, pp. 1–5, doi: 10.1109/ESTC48849.2020.9229859.

[80] C. Lenz, S. Ziesche, A. Schletz, H. L. Bach, and T. Erlbacher, "Real embedding process of SiC devices in a monolithic ceramic package using LTCC technology," in *Proc. IEEE 8th Electron. Syst.-Integration Technol. Conf.*, 2020, pp. 1–5, doi: 10.1109/ESTC48849.2020.9229653.

[81] C. Lenz et al., "Development and characterization of a monolithic ceramic pre-package for SiC-semiconductor devices based on LTCC technology," in *Proc. IEEE 9th Electron. Syst.-Integration Technol. Conf.*, 2022, pp. 62–66, doi: 10.1109/ESTC55720.2022.9939430.

[82] S. Ziesche, K. Reinhardt, J. Varghese, B. Manhica, and A. Schletz, "Ceramic embedding of SiC-semiconductor using cofiring technology," in *Proc. 24th Eur. Microelectron. Packag. Conf. Exhib.*, 2023, pp. 1–5, doi: 10.23919/EMPC55870.2023.10418439.

[83] A. Forte, R. Giofrè, W. Ciccognani, A. Serino, and E. Limiti, "A C-band two-stage MMIC GaN power amplifier for radar applications," in *Proc. 19th Conf. Ph.D Res. Microelectron. Electron.*, 2024, pp. 1–4, doi: 10.1109/PRIME61930.2024.10559724.

[84] F. Yang, K. Yin, H. Zhao, Y. Zhao, J. Liu, and S. Yang, "High power high efficiency solid state power amplifier used in space," *Chin. Space Sci. Technol.*, vol. 43, no. 2, pp. 55–62, 2023.

[85] Q. Jia et al., "Weakening the silicate network through six-coordinated magnesium to achieve a high degree of crystallization of β-CaSiO3 in calcium borosilicate glass ceramics for 5G application," *Ceram. Int.*, vol. 50, no. 11, pp. 20186–20193, Jun. 2024, doi: 10.1016/j.ceramint.2024.03.142.

[86] N. Jaziri, A. Schulz, H. Bartsch, J. Müller, and F. Tounsi, "A novel 2-in-1 heat management and recovery system for sustainable electronics," *Energy Convers. Manage.*, vol. 303, 2024, Art. no. 118171, doi: 10.1016/j.enconman.2024.118171.

[87] Z. Xiangzhao, Z. Santuan, L. Guiwu, X. Ziwei, S. Haicheng, and Q. Guanjun, "Review on brazing of high volume faction SiCp/Al composites for electronic packaging applications," *Rare Metal Mater. Eng.*, vol. 46, no. 10, pp. 2812–2819, 2017, doi: 10.1016/S1875-5372(18)30012-2.

[88] H. Yu, L. Jiaqin, and W. Yucheng, "Latest research progress of SiCp/Al composite for electronic packaging," *Rev. Adv. Mater. Sci.*, vol. 62, no. 1, 2023, Art. no. 20230158, doi: doi:10.1515/rams-2023-0158.

[89] C. Jiang et al., "Achieving high-efficiency electrically insulating ceramic layer formed on SiCp/Al composite by bipolar pulsed PEO for novel integrated strategy," *Surf. Coatings Technol.*, vol. 444, 2022, Art. no. 128692, doi: 10.1016/j.surfcoat.2022.128692.

[90] S. Ren, X. Qu, J. Guo, X. He, M. Qin, and X. Shen, "Net-shape forming and properties of high volume fraction SiCp/Al composites," *J. Alloys Compounds*, vol. 484, no. 1, pp. 256–262, 2009, doi: 10.1016/j.jallcom.2009.04.074.

[91] A. Maizeray et al., "Effects of dispersed α-Al2O3 particles into a cold-sprayed aluminium coating on its subsequent oxidation by the PEO process," *Surf. Coatings Technol.*, vol. 482, 2024, Art. no. 130713, doi: 10.1016/j.surfcoat.2024.130713.

[92] C. Jiang et al., "Rational design of compact ceramic coating on SiCp/Al composites by tailoring soft sparking discharge of plasma electrolytic oxidation," *Surf. Coatings Technol.*, vol. 466, 2023, Art. no. 129578, doi: 10.1016/j.surfcoat.2023.129578.

[93] C. Jiang et al., "A hBN/B-Si-Al-O-glass composite coating growth on SiCp/Al composite using one-step PEO with nanoparticle addition for outstanding electrical insulation performance," *Surf. Coatings Technol.*, vol. 475, 2023, Art. no. 130147, doi: 10.1016/j.surfcoat.2023.130147.

[94] C. Jiang et al., "Effects of negative voltage on microstructure, electrical insulating, anti-corrosion, and thermal physical performance of plasma electrolytic oxidation coating on SiCp/Al composite," *Appl. Surf. Sci.*, vol. 636, 2023, Art. no. 157789, doi: 10.1016/j.apsusc.2023.157789.

[95] J. Liang and N. Shigekawa, "Direct bonding of diamond and dissimilar materials for fabricating high performace power devices," in *Novel Aspects of Diamond II: Science and Technology*, S. Mandal and N. Yang, Eds. Berlin, Germany: Springer-Verlag, 2024, pp. 237–268.

[96] S. Kanda et al., "Fabrication of diamond/Cu direct bonding interface for power device applications," *Japanese J. Appl. Phys.*, vol. 59, 2020, Art. no. SBBB03, doi: 10.7567/1347-4065/ab4f19.

[97] Y. Zhong et al., "Heterogeneous integration of diamond-on-chip-on-glass interposer for efficient thermal management," *IEEE Electron Device Lett.*, vol. 45, no. 3, pp. 448–451, Mar. 2024, doi: 10.1109/LED.2024.3351990.

[98] J. Schöne, W. Beckert, B. Matthey, and M. Herrmann, "Modelling of the microstructure and thermal conductivity of SiC-bonded diamond materials," *Open Ceram.*, vol. 18, 2024, Art. no. 100594, doi: 10.1016/j.oceram.2024.100594.

[99] Z. Zhang, X. He, T. Zhang, P. Liu, and X. Qu, "Preparation of bimodal-diamond/SiC composite with high thermal conductivity," *J. Eur. Ceram. Soc.*, vol. 44, no. 2, pp. 643–650, 2024, doi: 10.1016/j.jeurceramsoc.2023.09.069.

[100] R. Prasher, "Thermal interface materials: Historical perspective, status, and future directions," *Proc. IEEE*, vol. 94, no. 8, pp. 1571–1586, Aug. 2006, doi: 10.1109/JPROC.2006.879796.

[101] B. Wei et al., "Thermal interface materials: From fundamental research to applications," *SusMat*, vol. 4, 2024, Art. no. e239, doi: 10.1002/sus2.239.

[102] X. Tian, M. E. Itkis, and R. C. Haddon, "Application of hybrid fillers for improving the through-plane heat transport in graphite nanoplatelet-based thermal interface layers," *Sci. Rep.*, vol. 5, no. 1, 2015, Art. no. 13108, doi: 10.1038/srep13108.

[103] P. Zhang, J. Zeng, S. Zhai, Y. Xian, D. Yang, and Q. Li, "Thermal properties of graphene filled polymer composite Thermal interface materials," *Macromol. Mater. Eng.*, vol. 302, no. 9, 2017, Art. no. 1700068, doi: 10.1002/mame.201700068.

[104] M. Shtein, R. Nadiv, M. Buzaglo, and O. Regev, "Graphene-based hybrid composites for efficient thermal management of electronic devices," *ACS Appl. Mater. Interfaces*, vol. 7, no. 42, pp. 23725–23730, 2015, doi: 10.1021/acsami.5b07866.

[105] R. L. Xu et al., "Thermal conductivity of crystalline AlN and the influence of atomic-scale defects," *J. Appl. Phys.*, vol. 126, no. 18, 2019, Art. no. 185105, doi: 10.1063/1.5097172.

[106] Z. Krstic and V. D. Krstic, "Silicon nitride: The engineering material of the future," *J. Mater. Sci.*, vol. 47, no. 2, pp. 535–552, 2012, doi: 10.1007/s10853-011-5942-5.

[107] N. Hegedüs, K. Balázsi, and C. Balázsi, "Silicon nitride and hydrogenated silicon nitride thin films: A review of fabrication methods and applications," *Materials*, vol. 14, no. 19, 2021, Art. no. 5658, doi: 10.3390/ma14195658.

[108] L. Li and Q. Cheng, "Anisotropic thermally conductive films based on two-dimensional nanomaterials," *Interdiscipl. Mater.*, vol. 3, no. 6, pp. 847–864, 2024, doi: 10.1002/idm2.12204.

[109] K. M. F. Shahil and A. A. Balandin, "Thermal properties of graphene and multilayer graphene: Applications in thermal interface materials," *Solid State Commun.*, vol. 152, no. 15, pp. 1331–1340, 2012, doi: 10.1016/j.ssc.2012.04.034.

[110] K. M. F. Shahil and A. A. Balandin, "Graphene–multilayer graphene nanocomposites as highly efficient thermal interface materials," *Nano Lett.*, vol. 12, no. 2, pp. 861–867, 2012, doi: 10.1021/nl203906r.

[111] Z. Li, Z. Xu, Y. Liu, R. Wang, and C. Gao, "Multifunctional non-woven fabrics of interfused graphene fibres," *Nat. Commun.*, vol. 7, no. 1, 2016, Art. no. 13684, doi: 10.1038/ncomms13684.

[112] K. Uetani, S. Ata, S. Tomonoh, T. Yamada, M. Yumura, and K. Hata, "Elastomeric thermal interface materials with high through-plane thermal conductivity from carbon fiber fillers vertically aligned by electrostatic flocking," *Adv. Mater.*, vol. 26, no. 33, pp. 5857–5862, 2014, doi: 10.1002/adma.201401736.

[113] H. Malekpour et al., "Thermal conductivity of graphene laminate," *Nano Lett.*, vol. 14, no. 9, pp. 5155–5161, 2014, doi: 10.1021/nl501996v.

[114] A. Ghozatloo, A. Rashidi, and M. Shariaty-Niassar, "Convective heat transfer enhancement of graphene nanofluids in shell and tube heat exchanger," *Exp. Thermal Fluid Sci.*, vol. 53, pp. 136–141, 2014, doi: 10.1016/j.expthermflusci.2013.11.018.

[115] M. Loeblein et al., "High-density 3D-boron nitride and 3D-graphene for high-performance nano–thermal interface material," *ACS Nano*, vol. 11, no. 2, pp. 2033–2044, 2017, doi: 10.1021/acsnano.6b08218.

[116] Y. Yao, J. Sun, X. Zeng, R. Sun, J.-B. Xu, and C.-P. Wong, "Construction of 3D skeleton for polymer composites achieving a high thermal conductivity," *Small*, vol. 14, no. 13, 2018, Art. no. 1704044, doi: 10.1002/smll.201704044.

[117] J. A. Cech Young, "13 - Next-generation CubeSats and SmallSats thermal control subsystem," in *Next Generation Cubesats and SmallSats*, F. Branz, C. Cappelletti, A. J. Ricco, and J. W. Hines Eds. Amsterdam, The Netherlands: Elsevier, 2023, pp. 307–328.

[118] V. Bianco, M. De Rosa, and K. Vafai, "Phase-change materials for thermal management of electronic devices," *Appl. Thermal Eng.*, vol. 214, 2022, Art. no. 118839, doi: 10.1016/j.applthermaleng.2022.118839.

[119] Y.-F. Zhang, D. Han, Y.-H. Zhao, and S.-L. Bai, “High-performance thermal interface materials consisting of vertically aligned graphene film and polymer,” *Carbon*, vol. 109, pp. 552–557, 2016, doi: 10.1016/j.carbon.2016.08.051.

[120] Z.-j. Huang et al., “Nacre-inspired flexible and thermally conductive phase change composites with parallelly aligned boron nitride nanosheets for advanced electronics thermal management,” *Composites Sci. Technol.*, vol. 255, 2024, Art. no. 110736, doi: 10.1016/j.compscitech.2024.110736.

[121] Q. Hu et al., “Oriented BN/silicone rubber composite thermal interface materials with high out-of-plane thermal conductivity and flexibility,” *Composites Part A, Appl. Sci. Manuf.*, vol. 152, 2022, Art. no. 106681, doi: 10.1016/j.compositesa.2021.106681.

[122] J. Hansson, T. M. J. Nilsson, L. Ye, and J. Liu, “Novel nanostructured thermal interface materials: A review,” *Int. Mater. Rev.*, vol. 63, no. 1, pp. 22–45, 2018, doi: 10.1080/09506608.2017.1301014.

[123] L. Zhang et al., “Metal telluride nanosheets by scalable solid lithiation and exfoliation,” *Nature*, vol. 628, no. 8007, pp. 313–319, 2024, doi: 10.1038/s41586-024-07209-2.

[124] T.-C. Chang, S. Lee, Y.-K. Fuh, Y.-C. Peng, and Z.-Y. Lin, “PCM based heat sinks of paraffin/nanoplatelet graphite composite for thermal management of IGBT,” *Appl. Thermal Eng.*, vol. 112, pp. 1129–1136, 2017, doi: 10.1016/j.applthermaleng.2016.11.010.

[125] T. Yang, P. V. Braun, N. Miljkovic, and W. P. King, “Phase change material heat sink for transient cooling of high-power devices,” *Int. J. Heat Mass Transfer*, vol. 170, 2021, Art. no. 121033, doi: 10.1016/j.ijheatmasstransfer.2021.121033.

[126] A. Hasan, H. Hejase, S. Abdelbaqi, A. Assi, and M. O. Hamdan, “Comparative effectiveness of different phase change materials to improve cooling performance of heat sinks for electronic devices,” *Appl. Sci.*, vol. 6, no. 9, p. 226, 2016, doi: 10.3390/app6090226.

[127] J. Yang et al., “Hybridizing graphene aerogel into three-dimensional graphene foam for high-performance composite phase change materials,” *Energy Storage Mater.*, vol. 13, pp. 88–95, 2018, doi: 10.1016/j.ensm.2017.12.028.

[128] D. Jamshideasli, “Heat transfer enhancement in thermal energy storage applications: A systematic review and data management in salts,” *J. Energy Storage*, vol. 46, 2022, Art. no. 103863, doi: 10.1016/j.est.2021.103863.

[129] C. Cárdenas-Ramírez, F. Jaramillo, and M. Gómez, “Systematic review of encapsulation and shape-stabilization of phase change materials,” *J. Energy Storage*, vol. 30, 2020, Art. no. 101495, doi: 10.1016/j.est.2020.101495.

[130] S. Krishnan, S. V. Garimella, and S. S. Kang, “A novel hybrid heat sink using phase change materials for transient thermal management of electronics,” *IEEE Trans. Compon. Packag. Technol.*, vol. 28, no. 2, pp. 281–289, Jun. 2005, doi: 10.1109/TCAPT.2005.848534.

[131] R. Kandasamy, X.-Q. Wang, and A. S. Mujumdar, “Transient cooling of electronics using phase change material (PCM)-based heat sinks,” *Appl. Thermal Eng.*, vol. 28, no. 8, pp. 1047–1057, 2008, doi: 10.1016/j.applthermaleng.2007.06.010.

[132] C. Ding, H. Liu, K. D. T. Ngo, R. Burgos, and G. Q. Lu, “A double-side cooled SiC MOSFET power module with sintered-silver interposers: I-design, simulation, fabrication, and performance characterization,” *IEEE Trans. Power Electron.*, vol. 36, no. 10, pp. 11672–11680, Oct. 2021, doi: 10.1109/TPEL.2021.3070326.

[133] D. D. Sharma, G. Pasdast, S. Tiagaraj, and K. Aygün, “High-performance, power-efficient three-dimensional system-in-package designs with universal chiplet interconnect express,” *Nat. Electron.*, vol. 7, no. 3, pp. 244–254, 2024, doi: 10.1038/s41928-024-01126-y.

[134] J. S. Knoll, G. Son, C. DiMarino, Q. Li, H. Stahr, and M. Morianz, “A PCB-embedded 1.2 kV SiC MOSFET half-bridge package for a 22 kW AC–DC converter,” *IEEE Trans. Power Electron.*, vol. 37, no. 10, pp. 11927–11936, Oct. 2022, doi: 10.1109/TPEL.2022.3177369.

[135] Z. Qi, Y. Pei, L. Wang, Q. Yang, and K. Wang, “A highly integrated PCB embedded GaN full-bridge module with ultralow parasitic inductance,” *IEEE Trans. Power Electron.*, vol. 37, no. 4, pp. 4161–4173, Apr. 2022, doi: 10.1109/TPEL.2021.3128694.

[136] A. Janabi et al., “Substrate embedded power electronics packaging for silicon carbide MOSFETS,” *IEEE Trans. Power Electron.*, vol. 39, no. 8, pp. 9614–9628, Aug. 2024, doi: 10.1109/TPEL.2024.3396779.

[137] R. Risch and J. Biela, “PCB-embedded packaging for ultra-fast switching of SiC MOSFETs,” in *Proc. 12th Int. Conf. Integr. Power Electron. Syst.*, 2022, pp. 1–7.

[138] Z. Dong, H. Yan, Y. Fan, X. Wu, and J. Zhang, “A 3-D integrated power module of GaN HEMTs based on silver sintering processes,” *IEEE Trans. Power Electron.*, vol. 39, no. 3, pp. 2932–2937, Mar. 2024, doi: 10.1109/TPEL.2023.3339759.

[139] L. Yang and W. G. H. Odendaal, “Measurement-based method to characterize parasitic parameters of the integrated power electronics modules,” *IEEE Trans. Power Electron.*, vol. 22, no. 1, pp. 54–62, Jan. 2007, doi: 10.1109/TPEL.2006.886615.

[140] B. Liu et al., “A low-thermal-stress double-sided cooling wire-bondless package structure of SiC power modules for high-temperature applications,” *IEEE Trans. Power Electron.*, vol. 39, no. 11, pp. 14741–14757, Nov. 2024, doi: 10.1109/TPEL.2024.3431589.

[141] S. Seal, M. D. Glover, and H. A. Mantooth, “3-D wire bondless switching cell using flip-chip-bonded silicon carbide power devices,” *IEEE Trans. Power Electron.*, vol. 33, no. 10, pp. 8553–8564, Oct. 2018, doi: 10.1109/TPEL.2017.2782226.

[142] L. Yang et al., “Electrical performance and reliability characterization of a SiC MOSFET power module with embedded decoupling capacitors,” *IEEE Trans. Power Electron.*, vol. 33, no. 12, pp. 10594–10601, Dec. 2018, doi: 10.1109/TPEL.2018.2809923.

[143] Z. Liang, “Planar-bond-all: A technology for three-dimensional integration of multiple packaging functions into advanced power modules,” in *Proc. IEEE Int. Workshop Integr. Power Packag.*, 2015, pp. 115–118, doi: 10.1109/IWIPP.2015.7295992.

[144] L. Wenduo, J. Dirker, and J. D. v. Wyk, “Power density improvement in integrated electromagnetic passive modules with embedded heat extractors,” *IEEE Trans. Power Electron.*, vol. 23, no. 6, pp. 3142–3150, Nov. 2008, doi: 10.1109/TPEL.2008.2005367.

[145] Y. Pascal, A. Abdedaim, D. Labrousse, M. Petit, S. Lefebvre, and F. Costa, “Using laminated metal foam as the top-side contact of a PCB-embedded power die,” *IEEE Electron Device Lett.*, vol. 38, no. 10, pp. 1453–1456, Oct. 2017, doi: 10.1109/LED.2017.2748223.

[146] E. C. W. d. Jong, B. J. A. Ferreira, and P. Bauer, “Toward the next level of PCB usage in power electronic converters,” *IEEE Trans. Power Electron.*, vol. 23, no. 6, pp. 3151–3163, Nov. 2008, doi: 10.1109/TPEL.2008.2004276.

[147] S. Moench et al., “PCB-embedded GaN-on-Si half-bridge and driver ICs with on-package gate and DC-link capacitors,” *IEEE Trans. Power Electron.*, vol. 36, no. 1, pp. 83–86, Jan. 2021, doi: 10.1109/TPEL.2020.3005621.

[148] F. Hou et al., “High power-density 3D integrated power supply module based on panel-level PCB embedded technology,” in *Proc. IEEE 68th Electron. Compon. Technol. Conf.*, 2018, pp. 1365–1370, doi: 10.1109/ECTC.2018.00208.

[149] F. Hou et al., “Microchannel Thermal Management system with two-phase flow for power electronics over 500 W/cm2 heat dissipation,” *IEEE Trans. Power Electron.*, vol. 35, no. 10, pp. 10592–10600, Oct. 2020, doi: 10.1109/TPEL.2020.2985117.

[150] F. Hou et al., “Review of packaging schemes for power module,” *IEEE J. Emerg. Sel. Topics Power Electron.*, vol. 8, no. 1, pp. 223–238, Mar. 2020, doi: 10.1109/JESTPE.2019.2947645.

[151] C. Hu et al., “The effect of thermal and moisture stress on insulation deterioration law of ionic contaminated high-voltage printed circuit board of electronic power conditioner,” *Energies*, vol. 15, no. 24, 2022, Art. no. 9616, doi: 10.3390/en15249616.

[152] L. Zhenxian, J. D. v. Wyk, and F. C. Lee, “Embedded power: A 3-D MCM integration technology for IPEM packaging application,” *IEEE Trans. Adv. Packag.*, vol. 29, no. 3, pp. 504–512, Aug. 2006, doi: 10.1109/TADVP.2006.879496.

[153] N. Zhu, H. A. Mantooth, D. Xu, M. Chen, and M. D. Glover, “A solution to press-pack packaging of SiC MOSFETs,” *IEEE Trans. Ind. Electron.*, vol. 64, no. 10, pp. 8224–8234, Oct. 2017, doi: 10.1109/TIE.2017.2686365.

[154] M. H. F. Lim, J. D. v. Wyk, and F. C. Lee, “Hybrid integration of a low-voltage, high-current power supply buck converter with an LTCC substrate inductor,” *IEEE Trans. Power Electron.*, vol. 25, no. 9, pp. 2287–2298, Sep. 2010, doi: 10.1109/TPEL.2010.2046913.

[155] J. Yin, Z. Liang, and J. D. v. Wyk, “High temperature embedded SiC chip module (ECM) for power electronics applications,” *IEEE Trans. Power Electron.*, vol. 22, no. 2, pp. 392–398, Mar. 2007, doi: 10.1109/TPEL.2006.889901.

[156] W. Chen, J. Jiang, A. H. Meda, M. S. Ibrahim, G. Zhang, and J. Fan, “A thin and low-inductance 1200 V SiC MOSFET fan-out panel-level packaging with thermal cycling reliability evaluation,” *IEEE Trans. Electron Devices*, vol. 70, no. 5, pp. 2268–2275, May 2023, doi: 10.1109/TED.2023.3263150.

[157] H. T. Le, Y. Nour, F. Jensen, A. Knott, A. Han, and Z. Ouyang, "Silicon power interposer technology (PIT) for integrated power converter," *IEEE Trans. Power Electron.*, vol. 38, no. 6, pp. 6755–6758, Jun. 2023, doi: 10.1109/TPEL.2023.3240357.
[158] C. A. Manier et al., "Wafer level embedding technology for packaging of planar GaN half-bridge module in high power density conversion applications," in *Proc. PCIM Europe; Int. Exhib. Conf. Power Electron., Intell. Motion, Renewable Energy Manage.*, 2018, pp. 1–8.
[159] P. Mackowiak, O. Wittler, T. Braun, J. Conrad, M. Schiffer, and M. Schneider-Ramelow, "Potentials of a SiC fan-out wafer level package for high power application," in *Proc. IEEE 9th Electron. Syst.-Integration Technol. Conf.*, 2022, pp. 45–48, doi: 10.1109/ESTC55720.2022.9939379.
[160] P. Mackowiak, K. Erbacher, M. Schiffer, H. D. Ngo, M. Schneider-Ramelow, and K. D. Lang, "Investigation of etching SIC VIAS for high power elctronics and harsh enviornment mems," in *Proc. IEEE 8th Electron. Syst.-Integration Technol. Conf.*, 2020, pp. 1–6, doi: 10.1109/ESTC48849.2020.9229659.
[161] P. Mackowiak, J. M. Köszegi, M. Schneider-Ramelow, and M. Schiffer, "TSiCV based Silicon carbide interposer technology," in *Proc. Smart Syst. Integration Conf. Exhib.*, 2023, pp. 1–6, doi: 10.1109/SSI58917.2023.10387967.
[162] J. M. Köszegi, P. Mackowiak, R. Stöcker, I. Ndip, M. Schiffer, and M. Schneider-Ramelow, "RF models for through SiC vias for highly integrated Interposer technology," in *Proc. Smart Syst. Integration Conf. Exhib.*, 2023, pp. 1–5, doi: 10.1109/SSI58917.2023.10387952.
[163] L. Böttcher, A. Ostmann, T. Löher, and M. Seckel, "Concepts for realizing high-voltage power modules by embedding of SiC semiconductors," in *Proc. 24th Eur. Microelectron. Packag. Conf. Exhib.*, 2023, pp. 1–6, doi: 10.23919/EMPC55870.2023.10418400.
[164] S. Mitarai et al., "Physical and thermal characteristics of the advanced package with glass core substrate," in *Proc. Int. Conf. Electron. Packag.*, 2024, pp. 173–174, doi: 10.23919/ICEP61562.2024.10535616.
[165] Q. Zhang, Y. Cao, and G. Wang, "Compact low-loss diplexer with stacked 2D and 3D structures using 3D glass-based advanced packaging technology," *AEU, Int. J. Electron. Commun.*, vol. 185, 2024, Art. no. 155425, doi: 10.1016/j.aeue.2024.155425.
[166] I. Kono, Y. Kometani, A. Kuroha, and Y. Kurita, "High precision and productivity bridge-die-last bonding process and its reliability for pillar- suspended bridge (PSB) architecture," in *Proc. IEEE 74th Electron. Compon. Technol. Conf.*, 2024, pp. 29–33, doi: 10.1109/ECTC51529.2024.00013.
[167] C. C. Lee, J. C. Chuang, C. T. Yang, C. I. I. Li, S. H. Lee, and S. H. Kuo, "Simulation and metrological applications for RDL patterning development of glass substrate," in *Proc. IEEE 74th Electron. Compon. Technol. Conf.*, 2024, pp. 990–995, doi: 10.1109/ECTC51529.2024.00160.
[168] T. Otsu et al., "Laser micro drilling of around 3 microns into Ajinomoto build-up film," in *Proc. IEEE 74th Electron. Compon. Technol. Conf.*, 2024, pp. 829–833, doi: 10.1109/ECTC51529.2024.00133.

Junwei Chen received the M.S. degree in materials science and engineering from the East China University of Science and Technology, Shanghai, China, in 2024. He is currently working toward the Ph.D. degree in electronic science and technology in the Academy for Engineering & Technology and Shanghai Engineering Technology Research Center for SiC Power Device, Fudan University, Shanghai, China.

His research interests include wide bandgap power semiconductor packaging and reliability, as well as advanced packaging technologies based on glass substrates.

Tiancheng Tian received the bachelor's degree in mechanical manufacturing and automation from the Hebei University of Engineering, Hebei, China, in 1999, and the master's degree in mechatronic engineering from Huaqiao University, Fujian, China, in 2006. He is currently working toward Ph.D. degree in electronic information engineering in Fudan University, Shanghai, China.

He has been engaged in the packaging design and process development of power devices. Especially in the past nine years, he has been working with Boschman Technologies B.V., a globally leading company, as a Senior Engineer focusing on the process mechanisms, equipment implementation, and engineering optimization during mass production of nano-silver pressure sintering and transfer molding for high-power power modules, as well as the development of new products and new processes.

Chao Gu received the M.S. degree in materials science and engineering from Tianjin University, Tianjin, China, in 2023. He is currently working toward the Ph.D. degree in electronic information engineering in Fudan University, Shanghai, China.

His research interests include wide band gap semiconductor power module design, packaging, reliability, and application.

Huidan Zeng received the B.S. and M.S. degrees in materials science and engineering from the South China University of Technology, Guangzhou, China, in 1998 and 2001, respectively, and the Ph.D. degree in materials science and engineering from the Shanghai Institute of Optics and Fine Mechanics, Chinese Academy of Sciences, Beijing, China, in 2004.

She is currently a Full Professor with the East China University of Science and Technology, Shanghai, China and a Marie Curie Scholar of European Union. Her research interests include functional glass, glass-ceramic and glass frit, including passivation/sealing glass of power devices, glass fiber and metal pastes (e.g., silver, copper) of MLCC/LTCC. She has published 150 peer-reviewed papers and holds 20 national patents.

Dr. Zeng is a member of the editorial committee of the Journal of Chinese Ceramic Society.

Fengze Hou (Senior Member, IEEE) received the Ph.D. degree in microelectronics engineering from the Department of Microelectronics, Delft University of Technology, Delft, The Netherlands, in 2020.

He is an Associate Researcher with the Institute of Microelectronics, Chinese Academy of Sciences, Beijing, China. He is also a Senior Engineer with the National Center for Advanced Packaging, Wuxi, China. His current research interests include thermal management, reliability, system integration, and SiC power module packaging.

Guoqi Zhang (Fellow, IEEE) received the Ph.D. degree in aerospace engineering from the Delft University of Technology, Delft, The Netherlands, in 1993.

He is the Chair Professor for "Micro/Nanoelectronics System Integration and Reliability," Delft University of Technology. He had worked for NXP Semiconductors as the Senior Director of Technology Strategy until 2009, Philips Research Fellow until May 2013. He authored/coauthored more than 400 scientific publications. His research interests include multilevel heterogeneous system integration and packaging, wide band gap semiconductors sensors and components, multiphysics and multiscale modeling of micro/nanoelectronics, and digital twin for mission critical multifunctional electronics components and systems.

Dr. Zhang serves as the Deputy Director for the European Center for Micro- and Nanoreliability (EUCEMAN), the Co-Chair of the Advisory Board of International Solid State Lighting Alliance (ISA), the Secretary General of the International Technology Roadmap of Wide bandgap Semiconductors (ITRW).

Jiajie Fan (Senior Member, IEEE) received the Ph.D. degree in industrial and systems engineering from Hong Kong Polytechnic University, Hung Hom, Hong Kong, in 2014.

He is currently a Youth Researcher with the Academy for Engineering & Technology and Shanghai Engineering Technology Research Center for SiC Power Device, Fudan University, Shanghai, China. His main research interests include prognostics and health management and wide bandgap power electronics packaging and reliability modeling.

Dr. Fan is an Associate Editor of IEEE Access.